Charles University

Faculty of Science

Study programme: Biology

Branch of study: Ecology

Bc. Tereza Vošická

Glacier's Legacy: Exploring the Impact of Glacier Retreat on Alpine Diatom Communities

Odkaz ledovců: Zkoumání vlivu ústupu ledovců na alpská společenstva rozsivek

Diploma thesis

Supervisor: Mgr. Kateřina Kopalová, Ph.D.

Consultants: Tyler Joe Kohler, Ph.D.; Mgr. Jan Kollár, Ph.D.

Prague, 2024

Prohlášení

Prohlašuji, že jsem závěrečnou práci zpracovala samostatně a že jsem uvedla všechny použité informační zdroje a literaturu. Tato práce ani její podstatná část nebyla předložena k získání jiného nebo stejného akademického titulu.

V Praze 12.12. 2024 Tereza Vošická

Aknowledgements

This thesis is dedicated to my beloved mother, Lucie Vošická, who sadly will never have the chance to see my scientific achievements. She made it her mission to ensure I could choose a path in life that truly fulfils me, and for that, I am forever grateful.

I am deeply thankful to my supervisor, Kateřina Kopalová, for her support and compassion during the challenging beginning of my master’s studies. Her kindness and encouragement provided me with much-needed strength during this difficult time.

I would like to extend special thanks to Jan Kollár, whose feedback improved my thesis in both content and presentation. His thoughtful suggestions were crucial to its completion.

I also owe a huge thanks to Tyler Kohler for being a constant source of advice and motivation throughout this process. His support has truly been available 24/7.

I extend my appreciation to Prof. Thomas Battin, Dr. Jade Brandani, Dr. Hannes Peter, Dr. Grégoire Michoud, Dr. Susheel Bhanu Busi, and other members of the ENSEMBLE team at EPFL for granting me access to their samples, data, and metadata. This research was made possible through funding from the Swiss National Science Foundation (grant CRSII5_180241), awarded to Prof. Battin. I am sincerely grateful for their contributions, which laid the foundation for this work.

Abstract

Diatoms play a crucial role in alpine stream food webs and biogeochemical cycles. However, the glaciers supplying water to some of these alpine streams (glacier-fed streams) are receding due to climate change, which will inevitably result in altered physicochemical conditions within these hydrological networks. Glacier-fed streams are harsh habitats, with low temperatures, high turbidity, and unstable substrata, and these habitats will likely be replaced by more stable precipitation and groundwater-fed streams in the future. This transition may shift diatom abundance and community composition, with some specialist diatom taxa potentially becoming extirpated, while generalist taxa become more abundant. Yet, little is known about how diatom communities will respond to such changes.

In this study, we use both traditional morphological and molecular methods to investigate diatom communities from alpine floodplains. Specifically, we sampled the benthic sediments of both glacier-fed streams and their corresponding non-glacial tributaries from three Alpine floodplains in Switzerland. We demonstrate that the transition from glacier meltwater inputs to precipitation and groundwater-based inputs will likely increase diatom community alpha diversity in alpine floodplains and lead to a significant restructuring of their communities. This restructuring and diversity increase are driven by the expansion of taxa associated with non-glacial streams, which, as shown in our research, outnumber glacier-fed specialists. While these changes may benefit a broad range of diatom taxa, including those on the red list of diatoms, they pose risks to species uniquely associated with glacier-fed environments. Furthermore, our findings underscore the complementary strengths and weaknesses of the different identification approaches, both in assigning taxonomic ranks and in analysing community-level patterns.

While emphasizing that glacier loss may lead to the complete disappearance of some streams and some diatom taxa, our study shows that the loss of glacier meltwater input in the prevailing streams will generally benefit glacial floodplain diatom communities by establishing conditions acceptable for a greater number and broader range of taxa. Additionally, we emphasise the value of combining multiple identification techniques (i.e., morphological and molecular methods) to capture the complexity of diatom taxonomy and to overcome the challenges posed by extreme alpine environments.

While further research is essential to explore the interactions between diatoms and other members of alpine stream microbial food webs to fully understand the ecological impacts of glacier retreat, our findings contribute to the development of targeted conservation strategies for these fragile ecosystems, while simultaneously encouraging innovative approaches to studying alpine stream microbiomes.

Keywords: *diatom assemblages, kryal streams, alpine stream food webs, glacier retreat, proglacial floodplains, microbial food web, diatom taxonomy, DNA barcoding, morphological identification*

Abstrakt

Rozsivky hrají klíčovou roli v potravních sítích a biogeochemických cyklech vysokohorských toků. Ledovce, které některé z těchto toků (toky ledovcové) napájejí, však v důsledku klimatických změn ustupují, což nevyhnutelně povede ke změnám fyzikálně-chemických podmínek. Ledovcové toky jsou náročná stanoviště s nízkými teplotami, vysokou turbiditou a nestabilním substrátem. V budoucnu budou pravděpodobně nahrazeny toky stabilnějšími, napájenými srážkami a podzemní vodou. Tento přechod může vést ke změnám hustoty a složení rozsivkových společenstev. Některé specializované taxony rozsivek mohou vyhynout, zatímco generalistické taxony se naopak stanou hojnějšími. Přesto dosud nevíme, jak na tyto změny rozsivková společenstva zareagují.

Tato studie kombinuje tradiční morfologické a molekulární určovací metody k výzkumu společenstev rozsivek alpských ledovcových údolí. Konkrétně porovnává bentické sedimenty z ledovcových toků a jejich přítoků bez přímého vlivu ledovcové vody ve třech švýcarských ledovcových údolích. Diplomová práce ukazuje, že přechod z toků napájených táním ledovců k tokům napájeným srážkami a podzemní vodou pravděpodobně zvýší jejich alfa diverzitu a zároveň povede k významné přestavbě jejich druhového složení. Tato změna složení a nárůst diverzity druhů jsou poháněny expanzí taxonů spojených s přítoky, které, jak ukázal náš výzkum, převyšují počtem specialisty na toky ledovcové. Zatímco tyto změny mohou být přínosné pro širokou škálu bentických rozsivek, včetně těch uvedených na seznamu ohrožených druhů, pro druhy úzce adaptované na podmínky ledovcových toků představují riziko. Naše výsledky dále zdůrazňují doplňující se silné a slabé stránky jednotlivých identifikačních metod a to jak při určování druhového složení, tak při zkoumání trendů na úrovni společenstev.

Přestože ztráta ledovců může vést k úplnému zániku některých toků a druhů rozsivek, naše studie ukazuje, že oslabení glaciálních vlivů povede díky rozšíření podmínek příznivých pro širší škálu druhů k nárůstu lokální diverzity (tj. alfa diverzity). Ztráta druhů specializovaných na drsné podmínky glaciálních toků ale zároveň povede k větší homogenizaci toků a tím potenciálně ke ztrátám diverzity na úrovni regionální (tj. beta a gama diverzity). Studie navíc poukazuje na důležitost kombinace různých metod určování taxonů (tj. morfologických a molekulárních) pro pokrytí složitosti taxonomie rozsivek a překonání výzev spojených s extrémním prostředím vysokohorských toků. Přestože další výzkum je nezbytný k prozkoumání interakcí mezi rozsivkami a dalšími členy potravních sítí vysokohorských toků, naše zjištění mohou přispět k rozvoji cílených strategií ochrany těchto ohrožených ekosystémů a zároveň podporují inovativní přístupy ke studiu jejich mikrobiomu.

Klíčová slova: *rozsivková společenstva, kryální toky, potravní sítě toků, ústup ledovců, ledovcová údolí, potravní sítě mikroorganismů, taxonomie rozsivek, DNA barcoding, morfologická identifikace*

Table of Contents

1 Introduction

Global warming is threatening the world's glacial ecosystems. Depending on the applied climate scenario, 22–51% of today's global glacial area could be lost by the end of the 21st century (Bosson et al., 2023). This trend is expected to be even more severe in the European Alps, where 90% of glaciers are smaller than 1 km² and thus more vulnerable to melting. Consequently, only 5–20% of the current glacial area in the Alps is projected to persist by 2100 (Zemp et al., 2006; Bosson et al., 2023; Rounce et al., 2023). This rapid change will inevitably alter the characteristics of alpine watersheds and their unique glacier-associated ecosystems. One such ecosystem type is glacier-fed streams, which transport glacier meltwater—along with fine particles eroded from surrounding rocks by glacial activity—to lower elevations, thereby creating a distinct habitat with critical importance for downstream communities (Sudlow et al., 2023).

The uniqueness of glacier-fed streams lies in their primary water source - glacier meltwater. For example, the freshly-melted ice keeps stream water temperatures just above 0 °C at the glacier snout, which then gradually increases on its way downstream. Since the intensity of glacier melt depends on solar heating, glacier-fed streams display both seasonal and diel fluctuations in discharge caused by changing meltwater inputs, creating hydrological peaks in summer and afternoons, respectively. It is during these peak discharges especially that intense water flow can cause the significant mobilisation of streambed sediments, decreasing channel stability, increasing turbidity, and scouring benthic communities (Brittain and Milner, 2001; Brown et al., 2003; Füreder and Niedrist, 2020; Sudlow et al., 2023). These conditions, along with low organic energy inputs from outside the stream (given that their riparian zones are above the treeline), make this environment particularly challenging to inhabit and often require specific life strategies and/or adaptations of its residents (Hieber et al., 2001; Brown et al., 2003; Gesierich and Rott, 2012; Sudlow et al., 2023).

Low allochthonous energy inputs make autochthonous primary production particularly important to the glacier-fed stream food webs. Alongside other photoautotrophs such as the cyanophytes (Cyanobacteria), green algae (Chlorophyta and Charophyta), and golden algae (Chrysophyceae), diatoms (Bacillariophyceae) are responsible for organic matter inputs and nutrient cycling in this otherwise nutrient-poor environment (Hieber et al., 2001; Rott et al., 2006; Clitherow et al., 2013; Brandani et al., 2022). Diatoms are unicellular brown microalgae possessing unique siliceous cell walls called 'frustules' (Round et al., 1990). Along with other diatom traits, such as high photosynthetic efficiency, lower temperature optimum for enzymes and anti-freeze proteins (Lyon and Mock, 2014), this frustule helps diatoms survive in the harsh conditions of glacier-fed streams by providing protection from mechanical stress and UV while also optimising capture of carbon dioxide and light (De Tommasi et al., 2017; Yang et al., 2023). These adaptations may help explain why the number of diatom species does not decline as rapidly with increasing glacier proximity as it does for many of the other photosynthetic groups mentioned previously (Rott et al., 2006). Consequently, diatoms hold a significant role in the functioning of glacier-fed stream ecosystems, making them worthy of further investigation. Yet, our knowledge of the diatom species composition in glacier-fed streams within the context of alpine stream networks is still limited.

Previous studies that focused on either the entire algal community (Hieber et al., 2001; Rott et al., 2006) or diatoms specifically (Robinson and Kawecka, 2005; Kawecka and Robinson, 2008; Gesierich and Rott, 2012; Fell et al., 2018) have reported a negative correlation between glacier proximity and both diatom density and richness in glacier-fed streams. According to Sudlow et al. (2023), this correlation is primarily driven by the intense physical disturbances characteristic of glacier-fed streams (i.e.

variation in discharge, streambed instability, suspended sediment loads), with light limitation, low temperatures, and oligotrophy likely playing a secondary role. As glaciers retreat, these hydrological disturbances will eventually become less intense and predictable, which is expected to result in community structure shifts within these streams. Specifically, small R-strategist diatom species with low biomass and strong attachment abilities (like species of the *Achnanthidium minutissimum* complex, which seem to thrive in these conditions) could be outcompeted by larger K-strategist diatoms and/or non-diatom taxa with various growth forms that are otherwise sensitive to high shear stress (Gesierich and Rott, 2012; Sudlow et al., 2023; Bert et al., 2024).

Yet, all the above-mentioned studies on glacier-fed stream diatoms relied on traditional morphological identifications (i.e., involving the direct visual examination of frustules under the light microscope) as the sole source of information about the diversity and structure of the resident diatom communities. However, diatoms are notorious for exhibiting extensive and widespread cryptic species diversity, meaning that multiple biological species are often morphologically indistinguishable (Mann and Evans, 2008; Pinseel et al., 2020). In addition, the harsh living conditions of glacier-fed streams generate considerable stress on the resident diatom communities. As a result, and combined with the high mass of fine glacier-derived sediment particles continuously deposited on the streambed, diatom communities are generally not very dense on the streambed nor in samples. This reality complicates their morphological evaluation through microscopy (Cantonati et al., 2001; Gesierich and Rott, 2012; Thies et al., 2013) and is perhaps a reason that glacier-fed stream diatoms have received relatively little study compared to other stream types in the past.

DNA barcoding can overcome some of these challenges by utilising short (300–600 bp) standardised DNA fragments known as “barcodes” to identify species (Hebert et al., 2003). This technique has been successfully used for identification of animal, plant, fungal, algal, and bacterial species through environmental sequencing, and its applications are rapidly expanding across diverse fields, including taxonomy, ecology, conservation biology, and even medicine and biotechnology (Fišer Pečnikar and Buzan, 2014; Rees et al., 2014; Ruppert et al., 2019; Kabiraj et al., 2022). Compared to morphological analysis—which in glacier-fed streams can be a tedious affair due to the above-mentioned challenges—DNA barcoding can be a less time-consuming and more cost-effective way of identifying resident species. Moreover, DNA barcoding is more consistent than traditional microscopy-based identifications, which can differ even among expert taxonomists (Kahlert et al., 2012). Furthermore, barcoding can identify species from incomplete or damaged material, is unaffected by different organismal life stages, and can often distinguish between cryptic species (Hebert and Gregory, 2005; Fišer Pečnikar and Buzan, 2014; Hubert and Hanner, 2015; Garlapati et al., 2019; Kollár et al., 2021). However, the success of DNA barcoding in identifying taxa by name is largely dependent on the quality and comprehensiveness of reference sequence databases, which are unfortunately still considerably underdeveloped for diatoms (e.g., Rimet et al., 2019). In addition, diatom species and genetic diversity is so extensive (e.g., Mann and Vanormelingen, 2013) that no single barcode marker, or even units of markers, can fully cover it, leading to a dual-barcode system that diatomology effectively utilizes today (Mann et al., 2010; Zimmermann et al., 2011; Vasselon et al., 2017). As a result, the most complete insight into the local diatom diversity is achieved through the combination of traditional morphology-based analysis and modern DNA barcoding methods (e.g., Mora et al., 2019).

The current dual-locus barcoding system of diatomology utilises regions in 18S rDNA and *rbc*L as barcode markers. The 18S rDNA (less frequently but more accurately called SSU rDNA) is a nuclear gene encoding the small subunit of eukaryotic ribosomes. It is popular due to its broad taxonomic coverage, ease of amplification, and effectiveness in resolving both higher and shallower taxonomic levels, stemming from the fact that it includes both conservative (stem) and variable (loop) regions

(Wang et al., 2014; Kabiraj et al., 2022). It has been applied to diatom phylogenetics since the turn of the millennium (Kooistra and Medlin, 1996; Medlin et al., 1996; Medlin and Kaczmarska, 2004; Sarno et al., 2005). For barcoding, the V4 or V9 region of the gene is usually targeted and is used frequently for environmental scanning of microeukaryotes (e.g., Amaral-Zettler et al., 2009; Stoeck et al., 2010; De Vargas et al., 2015). For diatomology, it was introduced primarily by Zimmermann et al. (2011) whose primers target a ca 400 bp long region including the V4. The greatest disadvantage of this marker is that there is no publicly curated diatom-specific 18S barcode database, complicating its utility.

The *rbc*L marker, in contrast, is a plastidial gene encoding the large subunit of the ribulose-bisphosphate carboxylase/oxidase (i.e., RuBisCO enzyme). It might be considered a more traditional barcode marker for photoautotrophic eukaryotes, including diatoms, as it is one of two standard markers designated for barcoding algae and plants (e.g., Hollingsworth et al., 2009). In addition, and unlike for 18S rDNA, the diatomological community has produced a curated *rbc*L reference sequence database (Diat.barcode database; Rimet et al., 2019), which is of course inexhaustive (including some 4,808 diatom *rbc*L sequences belonging to >1,000 species and varieties in the latest 11.1 version) compared to the enormous species diversity of diatoms (i.e., >18,000 described and >100,000 estimated species; Mann and Vanormelingen, 2013; Guiry, 2024). Nonetheless, the resource still provides a great advantage compared to the uncurated 18S rDNA databases.

Given the distinct strengths and challenges of these individual approaches, a combined methodology offers a more robust framework for investigating diatom assemblages. The aim of this study is to compare and contrast diatom assemblages taken from glacier-fed streams (GFSs) and their corresponding non-glacier-fed tributaries (TRIBs) using a combination of molecular and morphological approaches. Assessing the differences between GFSs and TRIBs provides a "space-for-time substitution" (Pickett, 1989), where TRIBs represent GFSs after the loss of their glacial meltwater inputs. As described above, GFSs are characterised by extreme conditions resulting from diurnally- and seasonally-dynamic glacial meltwater inputs. In contrast, TRIBs are primarily fed by precipitation and groundwater, and are therefore warmer, less turbid, and overall more stable (Sudlow et al., 2023). By sampling across three glacial floodplains in Swiss Alps, we here assess the influence of both stream type and glacial floodplain of origin on structuring benthic diatom communities. By combining the three methods, we can take advantage of their complementarity, minimize their individual limitations, and obtain a more accurate and complete picture of diatom diversity, while also comparing their effectiveness and current applications.

While we anticipate that both stream type and glacial floodplain of origin will significantly influence diatom community structure, we hypothesize that stream type will have a greater impact in driving these differences. Specifically, we expect TRIBs to exhibit higher diversity due to their less harsh and more stable environmental conditions. Conversely, we hypothesize that species composition, based solely on presence-absence data, will be more similar between different stream types within the same glacial floodplain than between streams of the same type across different floodplains. Furthermore, we expect that both stream types will host species significantly associated with their respective environments, with a greater number of indicator species found in tributaries, reflecting their anticipated higher alpha diversity.

This study aims to improve our understanding of the ecological changes that proglacial floodplain streams may undergo in response to climate change and contribute to the development of effective conservation strategies for preserving these unique, vulnerable, and rapidly diminishing habitats.

2 Materials and Methods

2.1 Study Sites and Sample Collection

The benthic sediment sample set used in this study was previously used for several other projects, including the mapping of the bacterial communities and phages (Brandani et al., 2023; Peter et al., 2024), as well as investigating cross-domain interactions, spatial patterns, and functional diversity in stream biofilms (Brandani et al., 2022; Michoud et al., 2023; Busi et al., 2024), and full details about the sampling can be found there. Briefly, samples were collected from three Swiss proglacial floodplains of three different glaciers – Otemma (OTE, 45.95E, 7.45N), Val Roseg (VAR, 46.39E, 9.84N) and Valsorey (SOY, 45.91E, 7.27N). A total of 262 sediment samples were collected: 112 from the GFSs and 150 from the TRIBs (Fig. 1). Both stream types were sampled within each floodplain across an area that extended ~1 km from each glacier snout. In these areas, stream sites were selected for collecting sediment samples. To maximize comparability across sites, sediments were taken from the benthic zone (up to ~5 cm deep in the streambed) and sieved (retaining only sediment grains from 0.25 to 3.15 mm) using flame-sterilised instruments. These samples were then transferred into cryovials, flash-frozen on dry ice, and kept frozen until analysis. Each site was sampled twice, once in June 2019 and once in

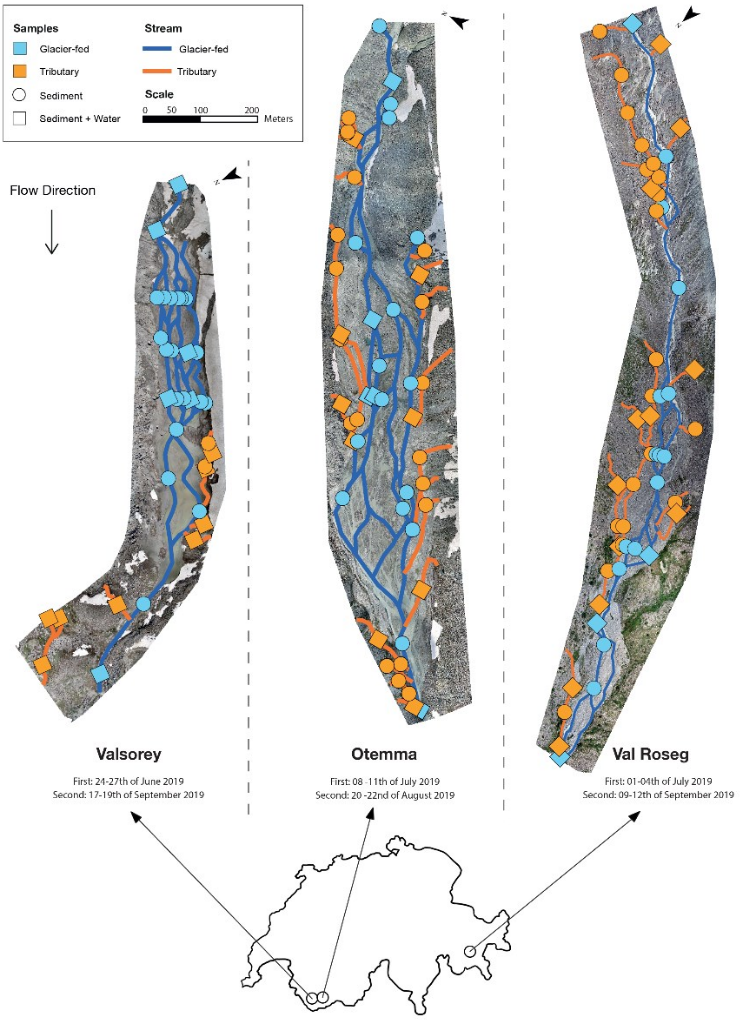

Figure 1: *Map of sampling sites in the floodplains of Valsorey [SOY], Otemma [OTE], and Val Roseg [VAR] glaciers in Switzerland. Glacier-fed streams [GFSs] are shown in blue, and tributary streams [TRIBs] in orange, flow direction is indicated by the arrow. The dates of sampling campaigns are listed below each glacier floodplain. The inset map shows the geographical locations of the sampling sites within Switzerland. Scale bars and north arrows are included for spatial reference (Brandani et al. 2022 - edited).*

August/September 2019. Since the above stated studies using these same samples did not find significant differences in community structure between these sampling periods, they were combined into one final dataset composed of all 262 samples from both samplings.

2.2 eDNA Extraction, Amplification, and Sequencing

In this study, the same eDNA extracts were utilised as in Brandani et al. (2022). These were generated through a phenol-chloroform DNA extraction method optimised for GFS samples (Busi et al., 2020), which was scaled down (to 0.5 g per extraction) to accelerate the sample processing prior to Polymerase Chain Reaction (PCR; Mullis et al., 1986) and Illumina sequencing. The final DNA concentration of all samples was adjusted to ≤ 3 ng/µl.

The targeted genetic markers were a ~300 bp barcode region of the nuclear 18S rDNA and a 263 bp barcode region of the plastid *rbc*L. The 18S rDNA data are the same as those used in Brandani et al. (2022). Here, the environmental 18S was amplified through PCR using general eukaryotic primers TAReuk454F (5′-CCAGCASCYGCGGTAATTCC-3′) and TAReukREV3 (5′-CTTTCGTTCTTGATYRA-3′; so called TAR primers), which target the gene's V4 loop region broadly utilised in DNA barcoding of microeukaryotes (Stoeck et al., 2010). The PCR products were verified on 1.5% (w/v) agarose gel, adjusted to ≤ 2–3 ng/µl, and sent for 300 bp paired-end sequencing to Lausanne Genomic Technologies Facility (LGTF, Switzerland, https://wp.unil.ch/gtf/).

For *rbc*L amplification and sequencing, the remaining eDNA extracts were sent to SEQme company (SEQme s.r.o., Czech Republic, https://seqme.eu/) along with negative extraction and positive amplification controls. The diatom specific primers used during this process consisted of equimolar mix of Diat_rbcL_708F_1 (5'-AGGTGAAGTAAAAGGTTCWTACTTAAA-3'), Diat_rbcL_708F_2 (5'-AGGTGAAGTTAAAGGTTCWTAYTTAAA-3') and Diat_rbcL_708F_3 (5'-AGGTGAAACTAAAGGTTCWTACTTAAA-3') as the forward primer, and mix of R3_1 (5'-CCTTCTAATTTACCWACWACTG-3') and R3_2 (5'-CCTTCTAATTTACCWACAACAG-3') as the reverse primer (Vasselon et al., 2017). In the samples with enough initial DNA concentration the DNA extracts were diluted to 2 ng/µl and subjected to 29-cycle PCR. Preparation of the amplicon libraries for *rbc*L was done according to the NovaSeq manufacturer's protocol and sequenced at 250 bp pair-end settings on the Illumina 6000 System platform.

2.3 Bioinformatic Processing

Sequence data were processed using QIIME 2 version 2022.8.0 (Bolyen et al., 2019). Paired-end reads were demultiplexed into individual samples, and primers were removed via the QIIME2 *cutadapt* plugin (Martin, 2011). Denoising to generate Amplicon Sequence Variants (ASVs) was executed with DADA2 (Callahan et al., 2016) within QIIME2. This bioinformatic pipeline includes quality-score-based filtering, correction of marginal sequence errors, elimination of chimeric sequences, merging of the paired-end reads, and dereplication of sequences. All ASVs with a total frequency of ≤ 10 reads across all samples were discarded.

For 18S, these steps resulted in a dataset composed of 23,287,302 eukaryotic reads distributed among 18,866 ASVs across 257 samples. To assign taxonomy, naive Bayes classifier (Bokulich et al., 2018) was trained on a custom diatom reference library built from GenBank (https://www.ncbi.nlm.nih.gov) using RESCRIPt (Robeson et al., 2021). The final number of sequences in the custom library was 18,305, with 9,120 diatom and 9,185 non-diatom sequences. The non-diatom 18S sequences were extracted from SILVA v.138.1 database (Quast et al., 2012) by randomly subsampling 20% of each present phylum, excluding diatoms. The classifier was then released upon our 18S dataset, and all non-diatom reads were discarded. As a result, the final 18S dataset consisted of 2,598,938 diatom reads distributed among 2,843 ASVs across 252 samples.

In contrast to 18S, *rbc*L is a protein-coding gene, and therefore ASVs containing stop codons within its longest open reading frame were discarded, on top of the steps described above. To assign taxonomy, the classifier was trained on Diat.barcode v. 11.1, a curated database containing 4,808 diatom *rbc*L sequences (Rimet et al., 2019). As a result, the *rbc*L dataset contained 5,625,482 diatom reads, distributed among 912 ASVs across 173 samples.

In both cases, confidence of the assignment was computed by 100 times bootstrapping a set of 8-mers found in a given ASV's sequence, and calculating the proportion of subsamples classified identically to the full sequence. A confidence threshold for retaining assignment to the given taxonomic level was set to 40% to limit artificial lumping under too high taxa (e.g., Bacillariophyceae). Its selection was empirical, resulting from the calibration with morphological data. In other words, the lowest taxon with confidence value ≥ 0.4 was kept as the final, discarding all the lower ones (whose confidence values were < 0.4). For example, if an ASV was assigned class, order, family, and genus names with confidence ≥ 0.4, and species name with < 0.4, the genus-level name is kept as the last confidently assigned level, making the ASV unassigned at species level.

2.4 Morphological Characterisation

Diatom communities were examined by microscope to (1) cover higher proportion of the total diatom diversity present on sites (see Introduction), (2) help calibrate the barcoding results, thus compensating for the insufficiency of current reference databases, (3) provide data on cell morphology that are unavailable through genetic analyses alone, and (4) make our study directly comparable to previous morphology-based studies on GFSs (e.g. Robinson and Kawecka, 2005; Fell et al., 2018; Bert et al., 2024). Due to the high concentration of fine sediment grains and low biomass in most samples, which severely complicated microscope analyses, a subset of samples with the highest expected concentrations of diatom cells based on the 18S sequencing results was selected for morphological characterization. This subset initially consisted of 79 samples: 21 from GFSs and 58 from TRIBs across the three floodplains.

The selected samples underwent a series of cleaning and concentration processes as described by Van der Werff, (1955). First, the benthic substrate was oxidised in 30% H_2O_2 for 3 to 5 days. Then, they were heated to ~100 °C for several hours to complete the oxidation. Following this, the surface layer of fine sediment, which contained the highest concentration of diatoms, was carefully removed. This layer was then subjected to a series of washes with distilled water. Specifically, the oxidised sediment was placed in a plastic 15 ml centrifuge tube, and distilled water was added to the marked maximum volume. The sample was then centrifuged at 3,500 rpm for 5 minutes. After the centrifugation, the supernatant was discarded. This washing procedure was repeated three times to ensure that all H_2O_2 is removed. After the final centrifugation, a small amount of distilled water was left in the tube. The concentrated solution was then dripped onto heated 22 × 60 mm coverslips and left to dry. The dried subsamples were permanently mounted in Naphrax® synthetic resin and allowed to cool before storing.

Morphological identification and cell measurements were performed using an Olympus BX43 light microscope (LM) equipped with an Olympus DP27 camera, with magnification up to 1000× under oil immersion. Where possible, 300 diatom valves were identified to the species level based on Krammer (1997), Krammer (2000) and Bey and Ector (2013). However, despite targeting a subset of the samples with the greatest potential diatom densities, the combination of high concentrations of fine particles and low cell density—particularly in the GFS samples—further limited the dataset for morphological characterization to 20 TRIB samples: seven from OTE, six from VAR, and seven from SOY. Of these, only 18 were successfully sequenced for 18S and *rbc*L, and these were used for comparison. The resulting relative abundance dataset primarily served as a reference for validating/calibrating the sequence data at the genus level.

Next, the most common species were examined using a JEOL IT800 Scanning Electron Microscope (SEM) to aid in the identification of small species. Prior to imaging, a small amount of the oxidized material was filtered and rinsed with deionized water using a vacuum pump and a 10 µm IsoporeTM polycarbonate membrane filter (Merck Millipore®). The filters were then mounted on aluminum stubs with double-sided carbon tape and coated with a 30 nm layer of platinum at 100 mA over 30 seconds using the BAL-TEC MED 020 modular high vacuum coating system.

2.5 Data Processing and Analysis

All the statistical analyses were performed in R (R Core Team, 2024) within the RStudio environment (Posit team, 2024). The data were transferred from QIIME2 to R using *qiime2r* package v. 0.99.6 (Bisanz, 2018) and analysed primarily in the *phyloseq* R package v. 1.84.0 (McMurdie and Holmes, 2013). Thus, unless a different package is explicitly specified, all functions mentioned below are from this package. To explore relationships between diversity saturation and sampling depth across all samples, the `rarecurve()` function within the *vegan* package (Oksanen et al., 2024) was used, plotting the rarefaction curves (Fig. 2), while *dplyr* package was utilised to manipulate the data (Wickham et al., 2023).

For comparability across, samples were rarefied to a sampling depth of 2,039 reads (based on the automatically detected threshold of diversity saturation, Fig. 2) with `rarefy_even_depth()` function (seed set randomly to 302 for reproducibility), discarding all samples below the threshold using `prune_samples()` function. After rarefaction, the number of samples was reduced from 252 to 126 for 18S and from 173 to 151 for *rbc*L. All subsequent analyses were conducted on the rarefied datasets.

Comparative barplots were created to display the top 12 genera of each dataset by relative abundance. For this, *microViz* (Barnett et al., 2021), *microbiome* (Lahti and Shetty, 2017), *colorspace* (Zeileis et al., 2020), *patchwork* (Pedersen, 2020), and *ggpubr* (Kassambara, 2020) packages were used to apply a coordinated colour scheme, adjust text size, and arrange plots.

Principal Coordinates Analyses (PCoA) were conducted using Bray-Curtis dissimilarity matrices (Bray and Curtis, 1957) to explore patterns in ASV composition. The analyses were performed with the `ordinate()` function and visualized using the `plot_ordination()` function from the *phyloseq* package in R. To test for significant differences in ASV composition, Permutational Multivariate Analyses of Variance (PERMANOVA) were conducted using the `adonis2()` function from the *vegan* package. Bray-Curtis dissimilarities were calculated, and significance was assessed with 999 permutations for each matrix. Permutational Analysis of Multivariate Dispersions (PERMDISP) was performed alongside each PERMANOVA to assess the homogeneity of multivariate dispersions, using the `betadisper()` function from the *vegan* package. All of these analyses were performed separately for two predictor variables: stream type and glacier floodplain, using both molecular datasets.

Differences in alpha diversity between the stream types were calculated using the `estimate_richness()` function and visualised as boxplots with the `plot_richness()` function from the *phyloseq* package. Since the assumptions of normality and homogeneity of variance were not met for our data, statistical significance between groups was assessed using the Wilcoxon Rank-Sum test, implemented with the `wilcox.test()` function from base R.

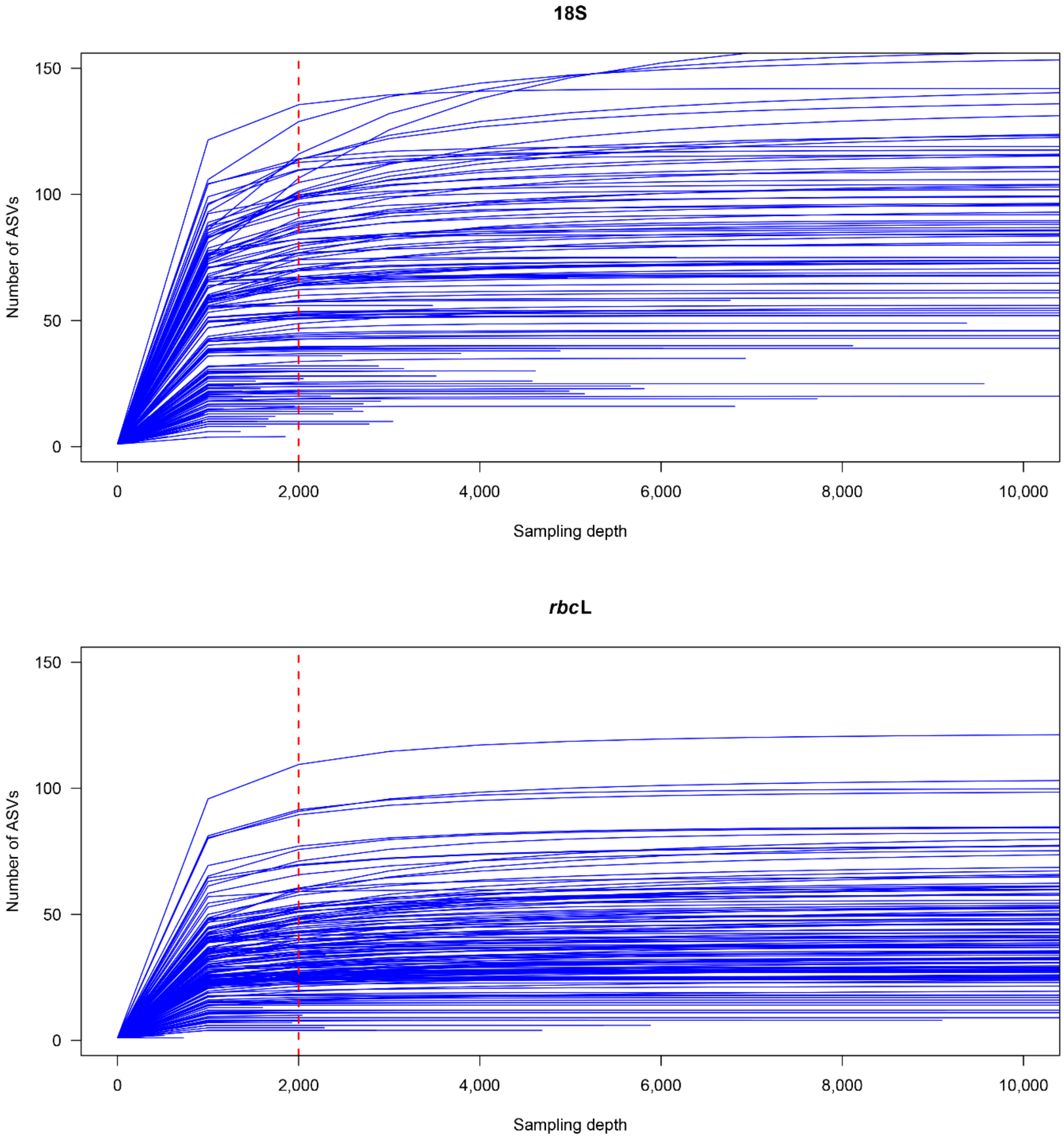

Figure 2: *Rarefaction curves for 18S (top) and rbcL (bottom) datasets. Each of the blue lines represents a single sample, showing the cumulative number of Amplicon Sequence Variants (ASVs) detected with increasing sampling depth (number of reads). The red dashed line detects the threshold where ASV counts begin to plateau, suggesting that this depth is sufficient to capture most of the diversity within most samples.*

The `upset()` function from the *UpSetR* package v. 1.4.0 (Gehlenborg, 2019) was used to display the distribution of ASVs across the stream types and floodplains. The similarities between ASV composition in the stream subsets were further tested using Jaccard similarity analysis with the `vegdist()` function from the *vegan* package. To examine genus-level distributions across streams, bubble plots were generated for both molecular and light microscopy data using the `ggplot()` function from the *ggplot2* package (Wickham, 2016). Finally, species significantly associated with specific stream types or floodplains were identified through Indicator Species Analysis with the `multipatt()` function from the *indicspecies* package (Cáceres and Legendre, 2009).

3 Results

3.1 Taxonomic Structure of the Communities

The rarefied 18S dataset contained a total of 2,395 ASVs in 126 samples, assigned to 103 species across 42 genera. Proportions of ASVs unidentified to species (39.7%) and genus (33.3%) were substantial even with the 0.4 confidence threshold (see *Materials and Methods*). The ASVs unidentified at species level contained 25.4% of all 18S reads, while those unidentified at genus level contained 14.0% of reads. In contrast, the *rbc*L marker recognized 825 ASVs in 151 samples, but identified comparable numbers of taxa, 139 species and 55 genera. Relatively lower proportions of ASVs could not be assigned to species (14.1%) or genus (8.2%), accounting for 2.7 and 0.8% of all *rbc*L reads, respectively.

To validate and calibrate the eDNA-based (18S and *rbc*L) taxonomic results, a subset of 18 TRIB samples covering all three floodplains was analysed under the LM to characterize communities based on morphology. A total of 35 genera were found based on morphology (Fig. 3 and 4), while in comparison, 37 genera were found in the corresponding sample set using 18S, and 42 genera were found with *rbc*L. In general, both markers match morphology reasonably well, but none of them perfectly (Fig. 5). For example, 18S better captures *Cocconeis* (Fig. 5, red), while overestimating *Navicula* (orange) when compared to *rbc*L and morphology. The *rbc*L misses *Cocconeis* (red) almost completely. On the other hand, *Caloneis* (brown) has higher relative abundances in the molecular barplots compared to morphological where it is nearly missed.

In general, TRIBs in the studied glacial floodplains were dominated by *Reimeria*, members of Achnanthidiaceae family (mainly *Achnanthidium* and *Psammothidium*), *Encyonema*, *Denticula*, *Cymbella*, *Amphora*, *Navicula*, *Planothidium*, *Nitzschia*, *Cymbopleura*, *Caloneis*, and *Gomphonema*, each accounting (on average) for at least 2% of their communities (Tab. 1). In relative terms, SOY TRIB communities were strikingly different from those from OTE and VAR, owing mainly to a considerably higher relative abundances of *Cocconeis* (red), *Denticula* (green), *Caloneis* (brown), and *Gomphonema* (grey). This alone suggests the existence of a regional pattern of diatom diversity across Alpine floodplains, and was further investigated (see below).

The dominant genera (≥2%) in GFSs (across 50 samples) showed similar patterns across both molecular markers. In both datasets, the most common genera were members of the Achnanthidiaceae family (*Achnanthidium* and *Psammothidium*), followed by *Reimeria*, *Gomphonema*, *Encyonema*, and *Nitzschia*. However, and similar to the 18 TRIB samples above, considerable differences in relative abundances were detected between the two genetic markers. For example, *Navicula* and *Cymbella* were prominent in the 18S data, while *Mayamaea* and *Pinnularia* featured prominently in the *rbc*L data. Notably, all four of these genera showed the highest representation in SOY, which similar to the TRIB subset above, stood apart from the other two floodplains. However, since these samples were not examined using LM, it is not possible to assess how these differences between methods align with the actual taxa composition.

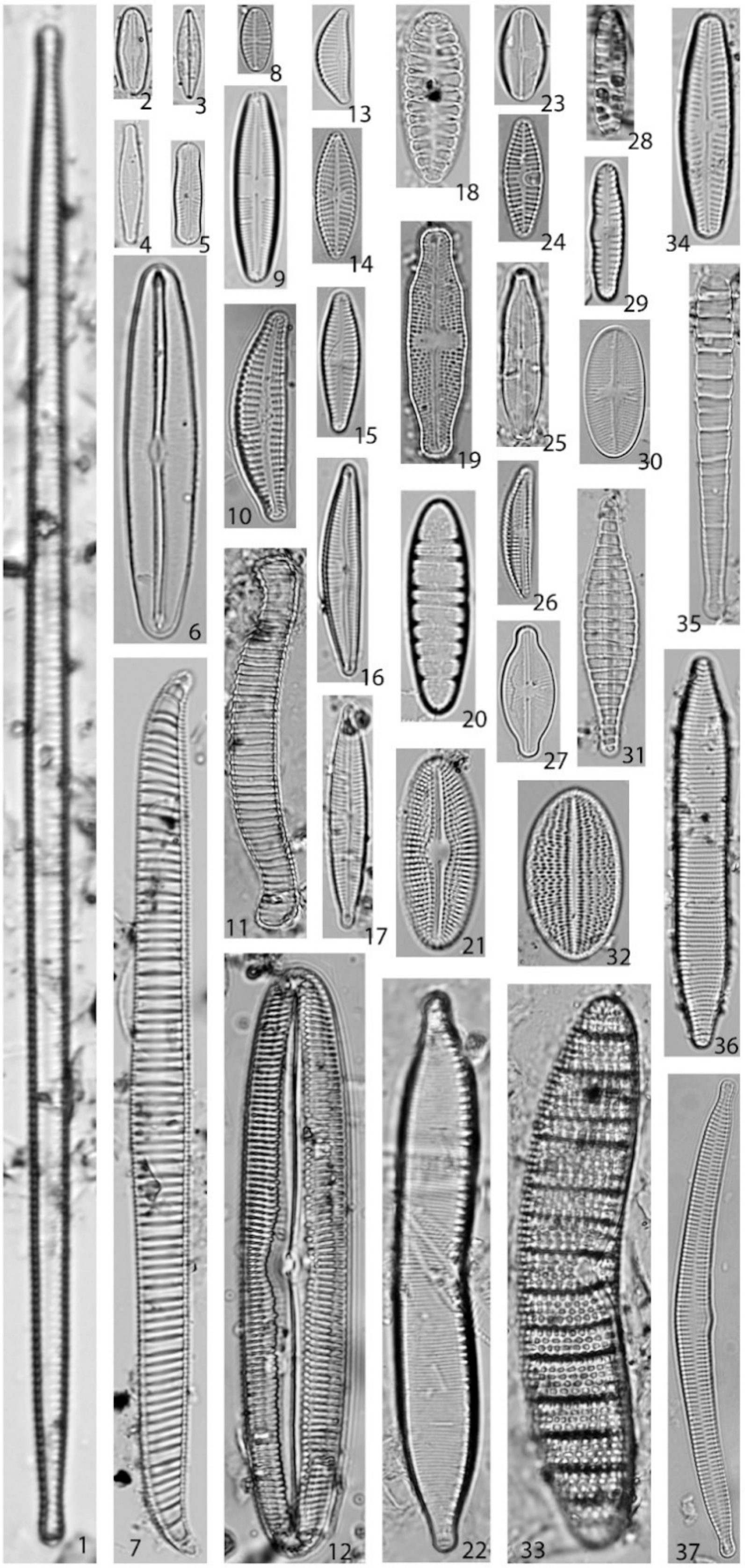

Figure 3: *Light microscopy (LM) micrographs of representative diatom species from each of the 37 genera obtained using morphological identification.*
(1) Fragillaria tenera, (2) Diadesmis perpusilla, (3) Adlafia miniscula, (4) Achnanthidium minutissimum, (5) Sellaphora ventraloides, (6) Frustulia vulgaris, (7) Rhopalodia gibba, (8) Geissleria acceptata, (9) Caloneis sp., (10) Cymbella excisiformis, (11) Eunotia arcubus, (12) Pinnularia subcommutata, (13) Encyonema brevicapitatum,(14) Navicula veneta, (15) Gomphonema cymbellicinum, (16) Delicata delicatula, (17) Encyonopsis cesatii, (18) Surirella pinnata (19) Luticola arctica, (20) Diatoma hyemalis, (21) Diploneis krameria (22) Hantzschia calcifuga, (23) Eucocconeis laevis, (24) Planothidium frequentissimum, (25) Stauroneis agrestis, (26) Amphora pediculus, (27) Cavinula pusio, (28) Staurosirella pinnata (29) Reimeria sinuate, (30) Psammothidium bioretii, (31) Denticula tenuis, (32) Cocconeis euglypta, (33) Epithemia adnate, (34) Cymbopleura sp., (35) Meridion circulare, (36) Nitzschia angustata, (37) Hannaea arcus. 10 µm bar in the bottom right corner was added for scale.

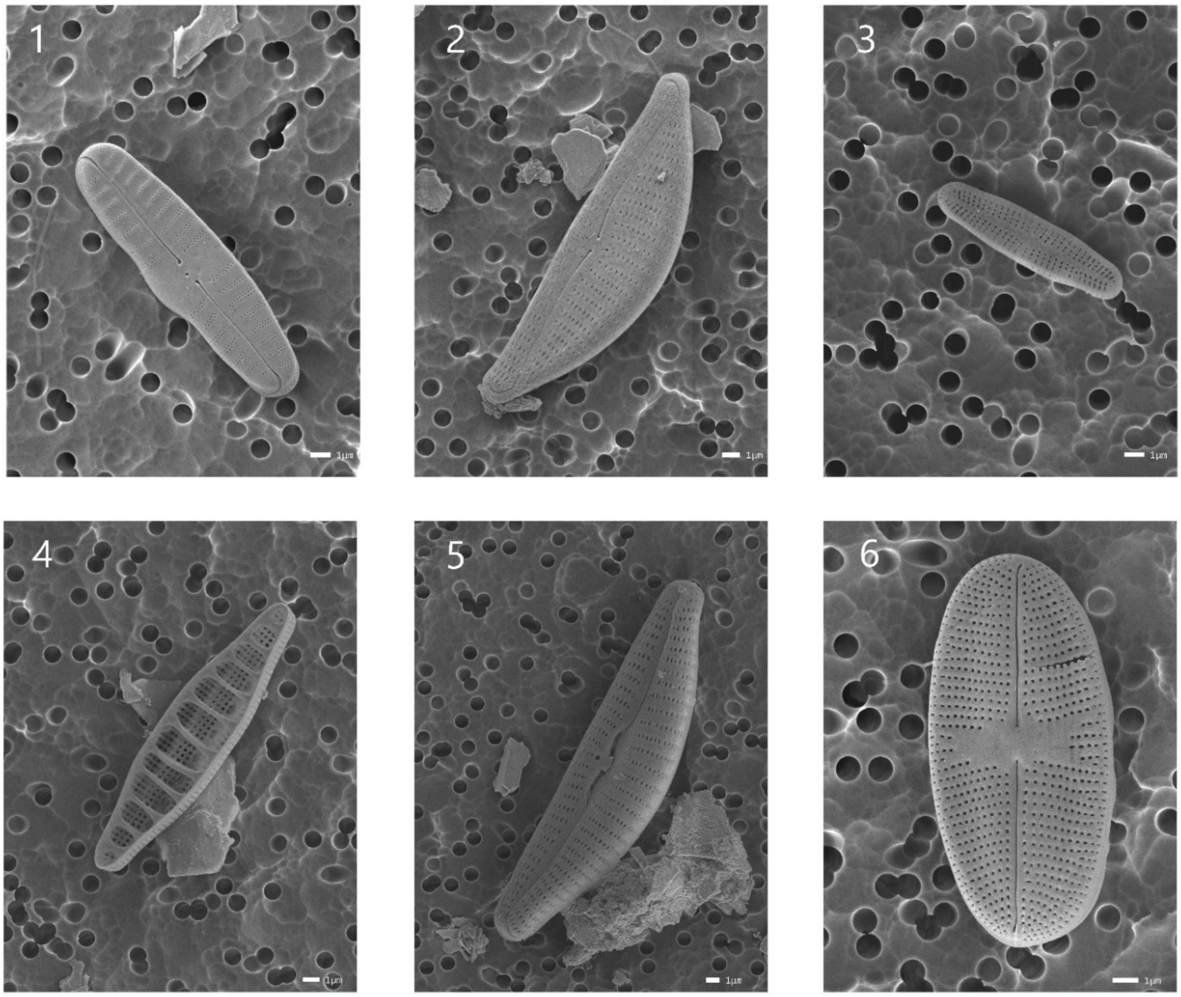

Figure 4: *Scanning Electron Microcopy photographs of the most common species for each of the top six diatom genera identified morphologically: Reimeria sinuata (1), Encyonema minutum (2), Achnanthidium minutissimum agg. (3), Denticula tenuis (4), Cymbella excissiformis (5), and Psammothidium bioretii (6). Each image includes a scale bar representing 1 µm.*

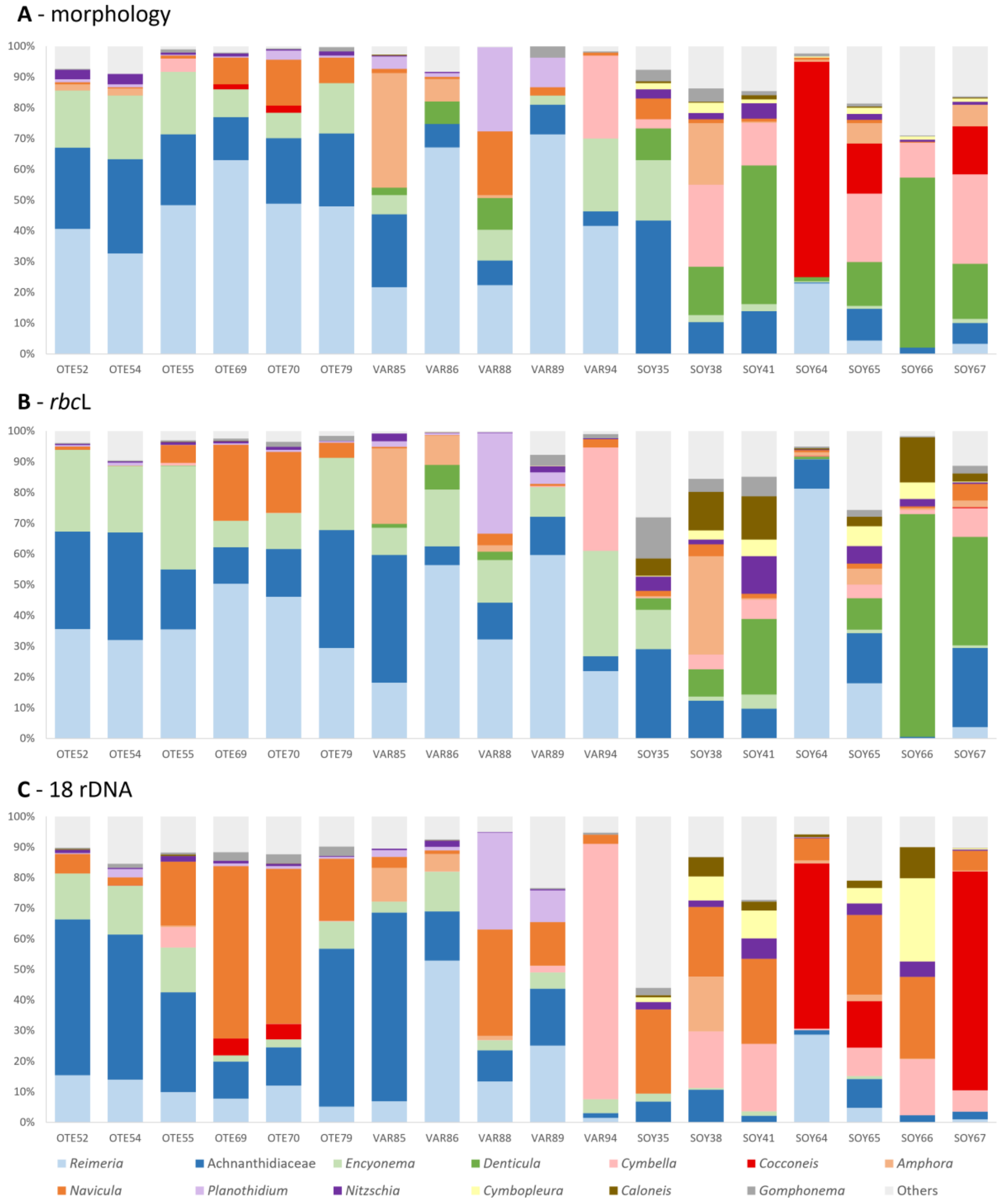

Figure 5 *Genus-level comparison of taxonomic structure (i.e. relative abundance) of communities in the subset of 18 tributary streams [TRIBs] across the three glacial floodplains (OTE - Otemma, VAR - Val Roseg, and SOY - Valsorey) as revealed by (A) morphology, (B) rbcL, and (C) 18S rDNA. Only genera with at least 2% average relative abundance in at least one of the three data kinds (i.e., morphology, rbcL, or 18S) are shown (color coded).*

__Table 1:__ Per sample average relative abundances of the dominant genera in the subset of 18 tributary streams [TRIBs] across the three datasets given as percentage ± standard deviation. A diatom genus was considered dominant when its average relative abundance reached 2% or more in at least in one of the datasets.

genus	**morphology**	***rbc*L**	**18S**
Reimeria	29.8 ± 25.0	29.0 ± 23.7	11.1 ± 13.5
Achnanthidiaceae	15.5 ± 11.3	18.4 ± 12.2	19.7 ± 20.2
Encyonema	9.1 ± 8.5	12.9 ± 11.3	5.3 ± 5.7
Denticula	10.0 ± 16.0	9.3 ± 18.5	0.0 ± 0.0
Cymbella	7.6 ± 11.1	3.4 ± 8.0	9.4 ± 20.0
Cocconeis	5.9 ± 16.8	0.0 ± 0.1	8.4 ± 20.4
Amphora	4.7 ± 9.6	4.4 ± 9.1	2.2 ± 4.8
Navicula	4.0 ± 5.8	4.4 ± 6.8	20.2 ± 16.6
Planothidium	2.7 ± 6.6	2.4 ± 7.7	2.8 ± 7.6
Nitzschia	1.3 ± 1.4	2.0 ± 3.0	1.6 ± 1.9
Cymbopleura	0.6 ± 1.0	1.2 ± 2.2	2.8 ± 6.7
Caloneis	0.2 ± 0.3	2.9 ± 5.2	1.3 ± 2.7
Gomphonema	1.1 ± 1.4	2.2 ± 3.3	0.9 ± 1.2
Others	7.5 ± 8.1	7.6 ± 8.5	15.0 ± 12.2

3.2 Influence of Environmental and Spatial Factors

3.2.1 Glacial Floodplain Influence

To investigate the influence of glacial floodplains of origin on diatom community composition, PCoA ordination plots were generated, grouping samples by glacial floodplain for both 18S and *rbc*L datasets (Fig. 6). These plots revealed a distinct separation among the floodplains, with diatom communities from SOY clustering distinctly apart from those in OTE and VAR, particularly in the *rbc*L plot. In contrast, diatom communities in OTE and VAR showed a more substantial overlap, especially in the *rbc*L ordination, indicating more similar community compositions between these two catchments. Notably, the *rbc*L data demonstrated a higher proportion of variability explained along Axis 1 by the glacier variable compared to the 18S data, suggesting a greater role of separation between VAR and the other two glaciers.

The glacial floodplain of origin had a significant effect on community composition in both the 18S and rbcL datasets, as demonstrated by Permutational Multivariate Analysis of Variance (PERMANOVA). The analysis indicated that the glacier variable accounted for approximately 14.6% of the total variance in the 18S dataset ($R^2 = 0.15$, $F = 10.47$, $p = 0.001$) and 20.6% in the rbcL dataset ($R^2 = 0.21$, $F = 19.17$, $p = 0.001$).

To investigate whether the influence of floodplain varies between stream types, separate PERMANOVA analyses were conducted for the GFS and TRIB data subsets. Community compositions were significantly different in both datasets. For the 18S data, the glacial floodplain of origin accounted for approximately 16% of the total variance in GFSs ($R^2 = 0.16$, $F = 2.61$, $p = 0.001$) and 18% in TRIBs ($R^2 = 0.18$, $F = 9.80$, $p = 0.001$). Similarly, the *rbc*L data indicated a significant floodplain effect, with around 24% of the total variance explained in GFSs ($R^2 = 0.24$, $F = 7.36$, $p = 0.001$) and 25% in TRIBs ($R^2 = 0.25$, $F = 06.04$, $p = 0.001$).

The PERMANOVA test was accompanied by a PERMDISP analysis, which checks for homogeneity of group dispersions. The test proved significant for both the 18S and *rbc*L sequenced data ($p = 0.001$), suggesting that significant results may also be partially due to unequal dispersions among groups from different glacial floodplains

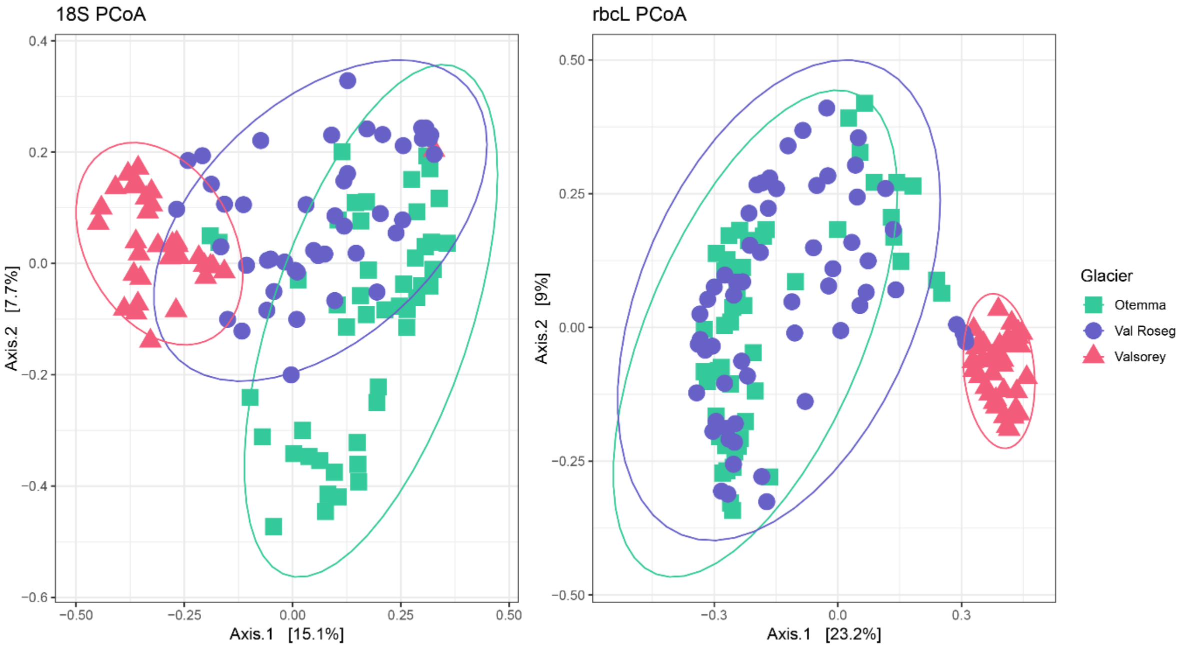

Figure 6: *PCoA ordination plots based on Bray-Curtis dissimilarities, comparing diatom community composition across Otemma [OTE], Val Roseg [VAR[, and Valsorey [SOY] glacial floodplain using two molecular markers - 18S (top) and rbcL (bottom). Shape and colour of each point indicate the origin of the sample it represents. Ellipses indicate 95% confidence intervals for each floodplain.*

3.2.2 Stream Type Influence

Given the significant differences in community structure observed among the glacial floodplains, the evaluation of differences between TRIBs and GFSs using PCoA was done for each floodplain separately. This analysis was performed using Bray-Curtis dissimilarities, consistent with the approach used for inter-floodplain comparisons (Fig. 7). The PCoA plots revealed differences between GFSs and TRIBs across all three floodplains, with varying degrees of separation. The distinction between stream types was most evident in SOY for the *rbc*L data (Fig. 7, panel E). Overall, the *rbc*L dataset shows clearer separation between stream types compared to 18S and explains a higher proportion of variance on Axis 1 across all catchments. To evaluate the statistical significance of these observed patterns, PERMANOVA analyses were performed separately for each glacier floodplain (Tab. 2).

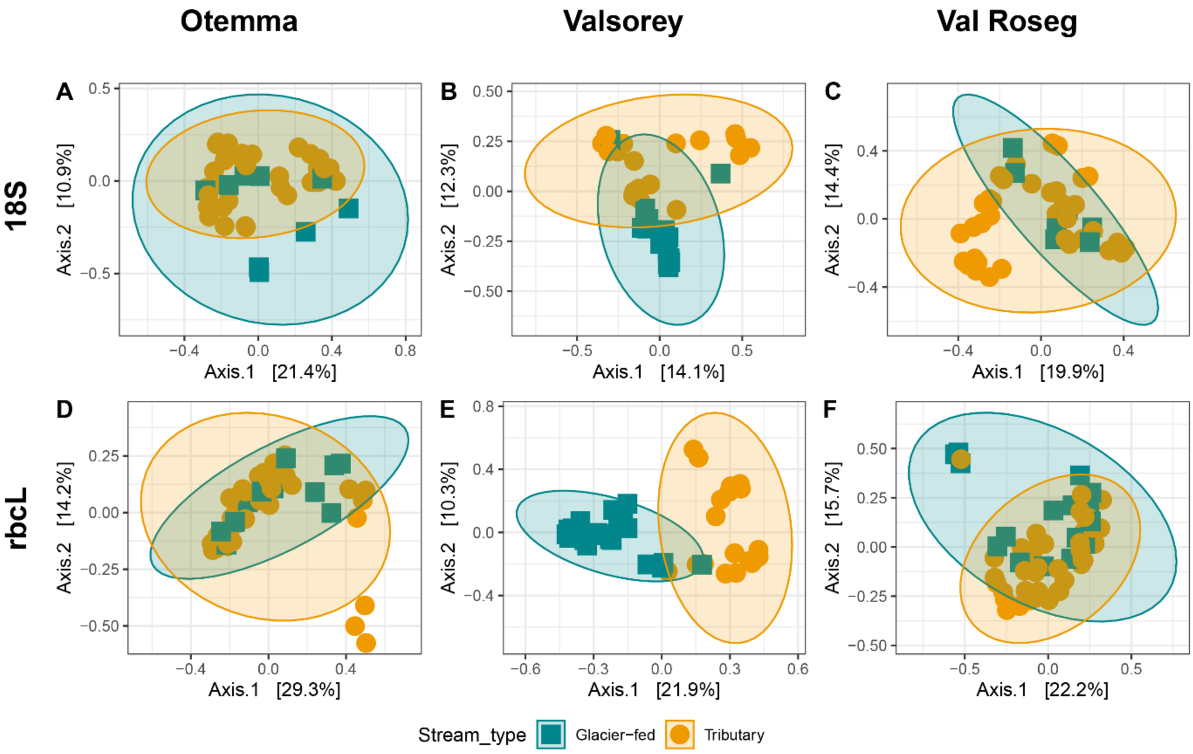

__Figure 7:__ Principle coordinate analysis (PCoA) using Bray-Curtis dissimilarities derived from 18S (top row) and rbcL (bottom row) sequenced data, with GFS (blue squares) and TRIB (orange circles) samples across three glacier catchments plotted: Ottema (OTE; A, D), Valsorey (SOY; B, E) and Val Roseg (VAR; C, F). Ellipses show 95% confidence intervals around the centroids of the GFS and TRIB groups. Axis 1 and Axis 2 represent the largest and second largest proportions of variability explained, respectively.

__Table 2:__ Results of PERMANOVA analyses testing for community composition differences between GFS and TRIB samples within each floodplain

Floodplain	**Marker**	***F*-value**	**R^2**	***p*-value**	**Significance**
OTE	18S	2.2936	0.0485	0.006	**
SOY	18S	2.9751	0.08506	0.001	***
VAR	18S	1.3557	0.03056	0.15	n.s.
OTE	*rbc*L	1.9659	0.03857	0.042	*
SOY	*rbc*L	8.3144	0.17952	0.001	***
VAR	*rbc*L	2.8053	0.04614	0.005	**

The PERMANOVA results confirmed that stream type was a significant factor influencing diatom community composition in five of the six datasets. The only exception was observed in the VAR floodplain sequenced with the 18S marker, where the p-value (p = 0.15) exceeded the significance threshold of 0.05. Among all datasets, the highest proportion of variance explained by stream type (R^2) was found in the SOY floodplain for both markers, consistent with the clearer separation of 95% confidence interval ellipses in the corresponding PCoA plots. Interestingly, the OTE floodplain was the only case where the 18S dataset explained more variability than the *rbc*L dataset.

To assess the validity of the PERMANOVA results, the PERMDISP test for homogeneity of group dispersions was performed. Significant differences in dispersion were found in the 18S datasets for OTE (p = 0.003) and SOY (p = 0.009), indicating that variability in these comparisons may be partially driven by uneven dispersions. Consequently, the PERMANOVA results for these comparisons should be interpreted cautiously. In contrast, the *rbc*L datasets exhibited no significant differences in dispersion ($p > 0.05$), providing greater confidence in their PERMANOVA outcomes.

PERMANOVA testing for the influence of stream type on the entire datasets was also conducted to facilitate comparison with the glacier floodplain effect. Both datasets proved significant effect of this variable. For the 18S dataset, stream type explained approximately 3% of the variability ($R^2 = 0.03$, $F = 3.42$, $p = 0.001$), while for *rbc*L, it accounted for about 5% ($R^2 = 0.05$, $F = 7.5$, $p = 0.001$). However, as with the tests for the floodplain effect, the PERMDISP analysis revealed significant differences in dispersion between groups, underscoring the need for cautious interpretation of these results.

3.3 Stream Type Diversity

To compare the overall diversity between stream types, alpha diversity indices were calculated and displayed in boxplots across studied floodplains for both sequencing datasets (Fig. 8).

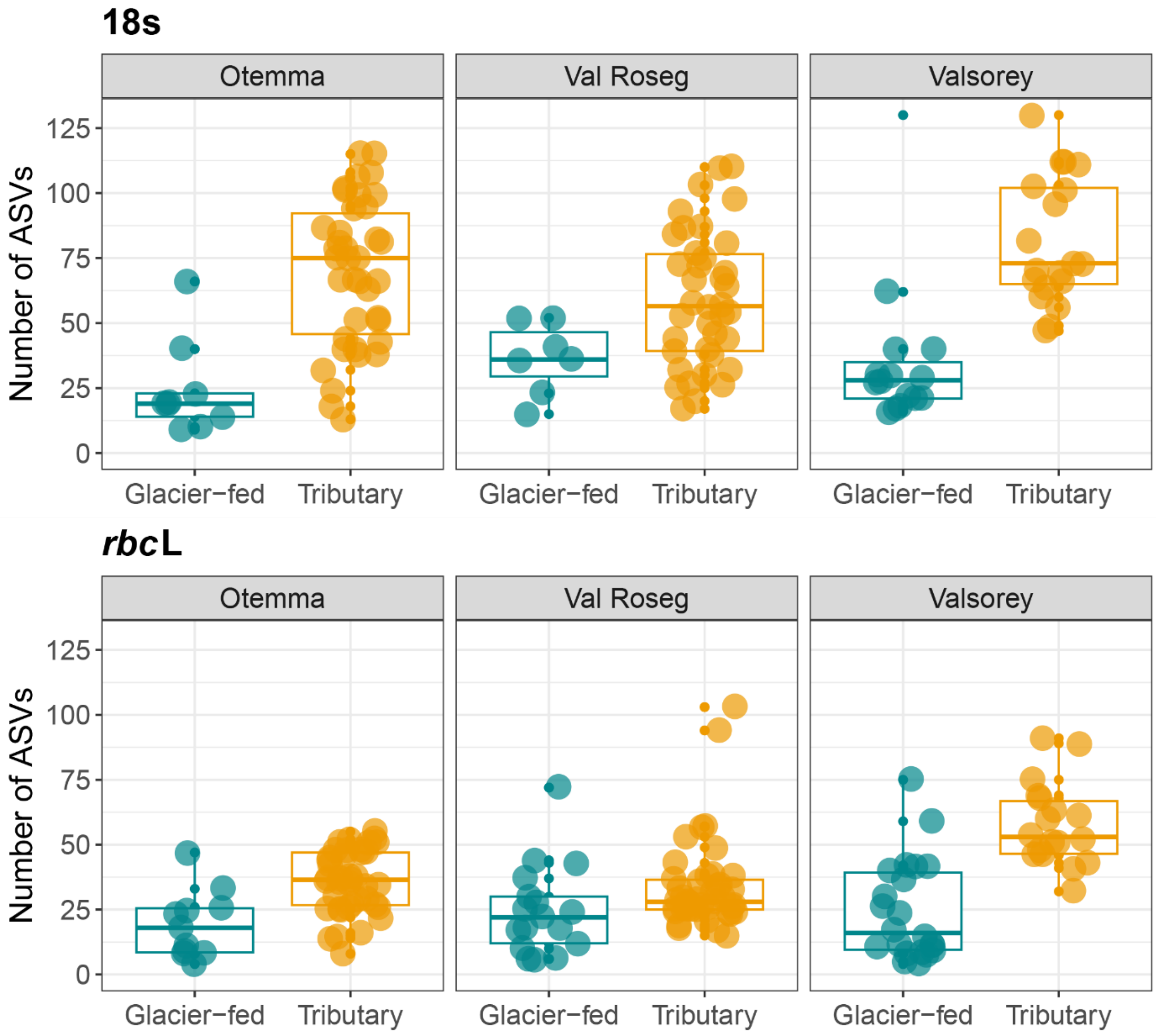

Figure 8: *Boxplots showing diatom ASV richness in GFSs (turquoise) and TRIBs (orange) across three glacier floodplains (Otemma [OTE], Val Roseg [VAR], Valsorey [SOY]), with the 18S dataset in the top row, and the rbcL dataset on the bottom.*

The median observed richness in TRIBs ranged from 56.5 to 75, while GFSs had lower medians ranging from 19 to 36. Similarly, in the *rbc*L dataset, the median observed richness in TRIBs (28 to 53) was higher than in GFSs (16 to 22). The interquartile ranges and standard deviations reflect greater variability in the TRIBs sequenced by 18S, whereas for *rbc*L, the variability in TRIBs is lower or similar to that in GFSs.

The boxplots highlighted clear differences in alpha diversity between GFSs and TRIBs across all glacier catchments and utilizing both sequencing methods. TRIBs consistently exhibited higher overall richness than GFSs. This pattern was particularly pronounced in the 18S dataset. The significance of these differences was further tested using the Wilcoxon rank-sum test (Tab.3).

Table 3: *Results of the Wilcoxon rank-sum test comparing alpha diversity (number of ASVs) between glacier-fed streams and tributaries for each glacial floodplain across both sequencing datasets.*

Floodplain	**Marker**	**Test statistic (*W*)**	***p*-value**	**Significance**
OTE	18S	31	1.6×10^{-4}	***
SOY	18S	22.5	3.37×10^{-5}	***
VAR	18S	59	0.025	*
OTE	*rbc*L	72.5	7.527×10^{-4}	***
SOY	*rbc*L	33.5	8.163×10^{-6}	***
VAR	*rbc*L	223	1.972×10^{-2}	*

The results confirmed that alpha diversity was significantly different between stream types, both across the entire dataset ($W = 405.5$, $p = 1.859^{-9}$ for 18S; $W = 1178$, $p = 1.004^{-7}$ for *rbc*L) and within each glacial floodplain. The lower significance level observed for VAR in both sequencing datasets aligned with the boxplots, where the medians for VAR were closer together compared to those of the other floodplains in both datasets.

3.4 Community Similarities Across Sites

The number of ASVs present in each subset of the data and in their combinations was visualised using the Upset plot (Fig. 6). The plots for both the 18S and *rbc*L data showed that most of the ASVs were specific to one of the six subsets of different stream types and floodplains only (63-561 ASVs in 18S and 35-162 ASVs in *rbc*L). The only exception was OTE GFS-specific ASVs in the 18S data, which ranked lower in the order. Both methods also indicated a high proportion of ASVs shared between both stream types within the same glacier catchment, and between OTE and VAR TRIBs. There was a moderate representation of ASVs shared between all six stream subsets (10 in 18S; 8 in *rbc*L data) and in all three TRIB subsets specifically (22 in 18S; 8 in *rbc*L).

The total number of ASVs within each of the six subsets differed significantly between the two methods. The 18S dataset showed an overall higher ASV counts and a greater distinction between GFSs and TRIBs. In contrast, the *rbc*L data displayed less pronounced differences between stream types, with an unexpectedly high ASV count observed in the ‘GFS SOY’ subset.

To further investigate the turnover of taxa between pairs of stream subsets, Jaccard similarity analysis (which, like the UpSet plot, is based on the presence or absence ASVs) was conducted (Fig. 10). For the 18S data, Jaccard similarity values were generally low across all six sample subsets, indicating limited overlap of present ASVs, which aligned with the higher ASV counts and greater specificity observed in the UpSet plot. In contrast, all subsets in the *rbc*L dataset exhibited higher Jaccard similarity values, especially among same catchment streams.

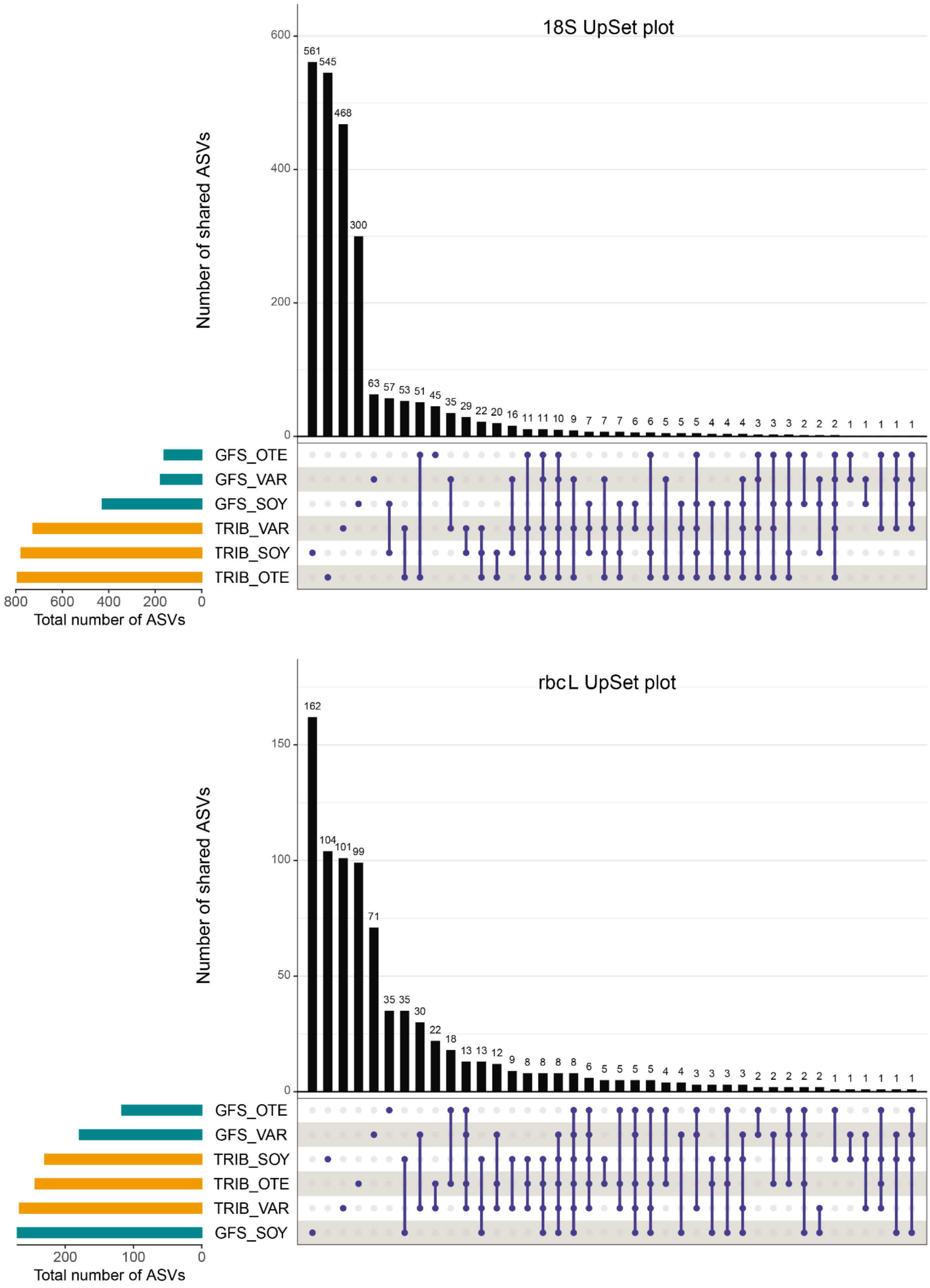

Figure 9: *UpSet plots showing the distribution of ASVs across sample subsets of glacier-fed Otemma [GFS_OTE], glacier-fed Val Roseg [GFS_VAR], glacier-fed Valsorey[GFS_SOY], tributary Otemma [TRIB_OTE], tributary Val Roseg [TRIB_VAR] and tributary Valsorey [TRIB_SOY]. Both datasets 18S (top) and rbcL (bottom) are displayed in separate plot. Vertical black bars represent the number of ASVs shared across the different subsets (indicated by blue dots) and their combinations (indicated by blue line connections). The horizontal bars showing glacier-fed streams in turquoise and tributary streams in orange, indicate the total number of ASVs in each of the subsets.*

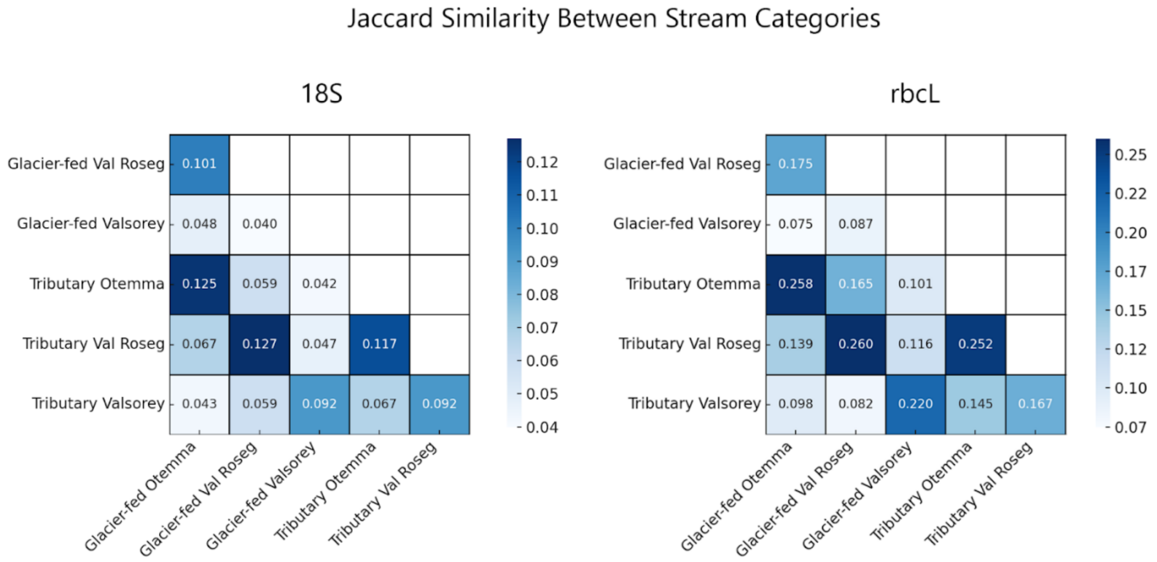

Figure 10: *Jaccard Similarity Between Stream Categories for 18S and rbcL Data. Heatmaps display the Jaccard similarity indices for diatom communities between pairs of stream categories based on ASV presence/absence data from 18S (left) and rbcL (right) sequencing. Higher values indicate greater overlap in ASV composition between subsets.*

Both methods showed high similarity between both stream types of same floodplains—especially in OTE and VAR— followed by the tributary streams of VAR and OTE, which corresponds with the UpSet plot results. GFSs generally showcased low similarity, except for the VAR and OTE pair, where the overlap was more pronounced.

3.5 Stream-type Specific Taxa

To explore taxonomic differences between floodplains and stream types, bubble plots of relative abundances were created for the dominant genera in each of the six sample subsets (Fig. 11). The sequencing data plots were accompanied by an LM data plot, displaying the genera composition in TRIBs to provide a comparison with physically observed diatoms (Fig. 12).

The plots suggest that the high-abundance genera are often present across all stream types and floodplains. These genera included *Achnanthidium, Encyonema, Navicula, Psammothidium* (with the exception of SOY in the LM plot), and *Reimeria* (absent in the SOY *rbc*L plot). A considerably high proportion of the displayed genera, such as *Cymbopleura, Diploneis, and Encyonopsis,* seemed to be associated with the SOY glacier floodplain specifically, while some other genera like *Frustulifera* or *Hannaea* conversely tended to be present in all streams except those associated with SOY. In the sequencing data, few genera exhibited a strong preference for a specific stream type.

Notably, certain genera, such as *Geissleria*, *Surirella*, and *Fragilaria*, revealed inconsistencies in distribution across the sample subsets, depending on the identification method. Additionally, some taxa, while substantially represented in two of the plots, were absent in the third. This can be seen with *Denticula* in the 18S plot, *Cocconeis* in the *rbc*L plot, *Frustulifera* in the LM plot, and several of others (Fig.12).

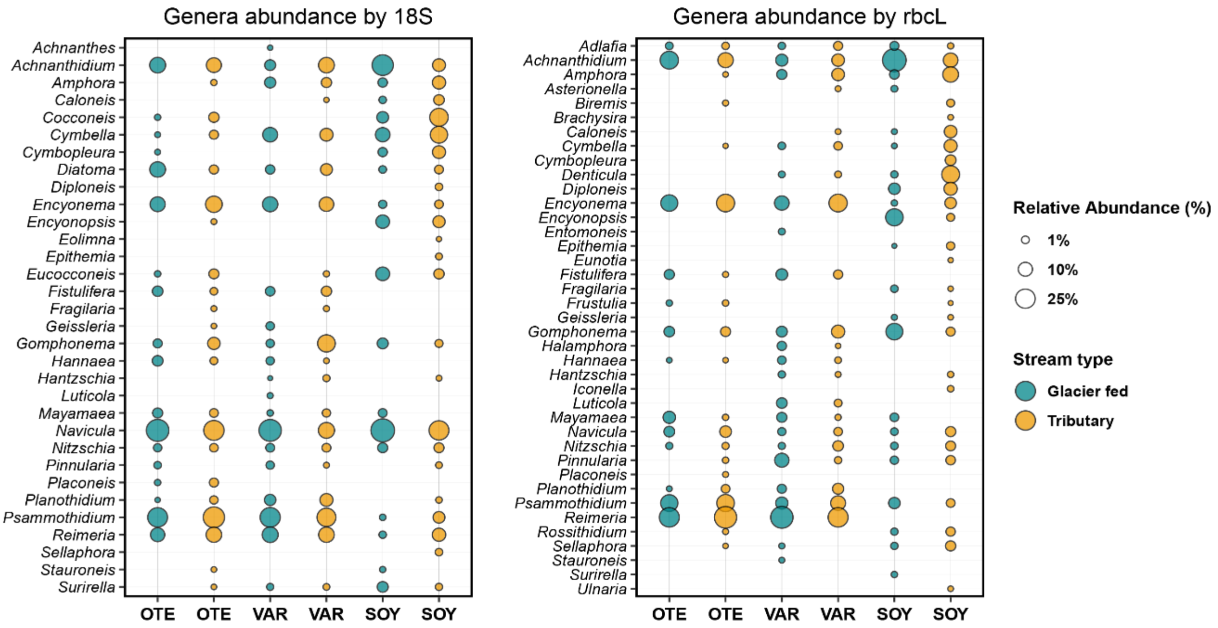

***Figure 11:** Bubble plots depicting genera with relative abundances >0.001 across different stream types in three catchments (Otemma [OTE], Val Roseg [VAR], Valsory [SOY]) for 18S (left) and rbcL (right) sequencing data. Bubble size represents the percentage abundance within glacier-fed (GFS; turquoise) and tributary (TRIB; orange) streams.*

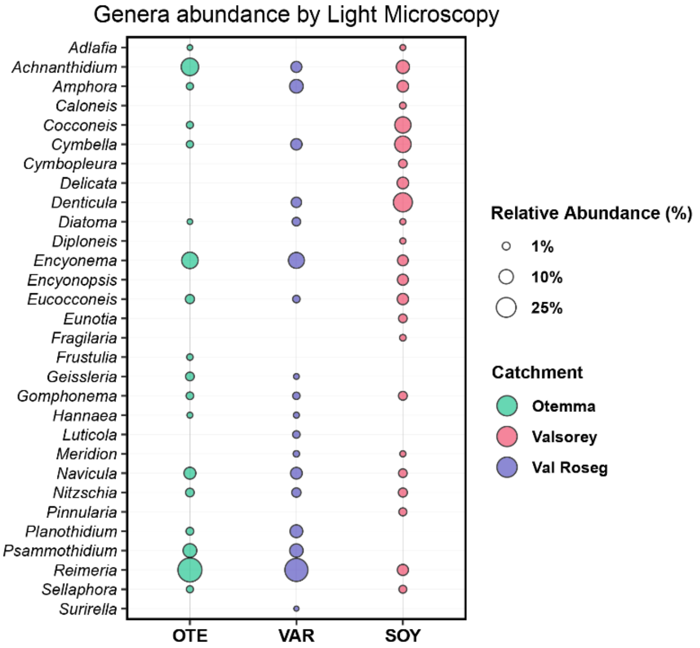

***Figure 12**: Bubble plot depicting genera with relative abundances >0.001 across three catchments: Otemma [OTE] (green), Val Roseg [VAR](purple), and Valsorey [SOY] (red) identified through light microscopy. Bubble size represents the percentage abundance within each catchment.*

The association with glacier floodplains was tested via Indicator Species Analysis (IndVal) to provide quantitative evidence for the patterns observed in the bubble plots. This analysis confirmed that genera appearing in only one of the glacier floodplains in the bubble plots, such as *Cymbopleura* in SOY, *Luticola* in VAR or *Placoneis* in OTE, were indeed significantly associated with that specific glacier.

The IndVal analysis identified far fewer floodplain-associated ASVs (212) in the *rbc*L dataset compared to the 18S dataset (363), particularly in the OTE and SOY floodplains, where less than half the ASVs identified by 18S were detected by *rbc*L.

IndVal was also applied to test for ASVs characteristic for either GFS or TRIB stream types. For the 18S data, 20 out of 2,395 detected ASVs were found to be significantly associated with GFSs, and 34 were found to be characteristic of TRIBs. Unlike in the IndVal results looking for floodplain-specific taxa, higher numbers were observed for the *rbc*L dataset: of 825 ASVs, 32 were associated with GFSs and 46 with TRIBs. ASVs with the strongest association to both stream types are listed in Tables 4 and 5.

It is important to note that several of the stream type-associated ASVs identified by IndVal were unassigned at the species level, including some of those with the highest significance. For 18S, 15 out of the 20 GFS-associated ASVs, and 11 out of the 34 TRIB-associated ASVs, remained unidentified. The rbc*L* dataset showed similar numbers, although with a lower proportion: 14 out of 32 ASVs for GFSs were unidentified, and 11 out of 46 ASVs for TRIBs.

Table 4: *Indicator Species Analysis results for top 20 species most strongly associated with glacier-fed streams [GFS] and tributaries [TRIBs] based on 18S data.*

	18S GFSs			**18S TRIBs**		
	ASV	**stat**	**p.value**	**ASV**	**stat**	**p.value**
1	NA 11	0.475066	0.005	*Reimeria sinuata*.7	0.720735	0.03
2	NA 70	0.438584	0.005	*Psammothidium papilio*.26	0.718074	0.03
3	NA 194	0.43856	0.01	*Gomphonema micropus*.10	0.712715	0.01
4	NA 600	0.40161	0.005	*Gomphonema parvulum*.2	0.675628	0.01
5	NA 71	0.400082	0.015	*Psammothidium papilio*.25	0.661317	0.005
6	*Navicula cryptotenella*.55	0.366016	0.035	NA 78	0.648886	0.005
7	NA 481	0.359211	0.005	*Encyonema silesiacum*.21	0.588348	0.025
8	NA 580	0.359211	0.005	*Planothidium lanceolatum*.6	0.565208	0.015
9	NA 196	0.357541	0.025	NA 375	0.542897	0.01
10	*Encyonopsis* sp.5	0.347951	0.015	*Encyonema silesiacum*.14	0.532032	0.035
11	*Achnanthidium* sp. 36	0.311086	0.02	*Planothidium frequentissimum*.2	0.523148	0.015
12	*Nitzschia cf. pusilla* .14	0.311086	0.03	*Reimeria sinuata*.16	0.522346	0.025
13	*Navicula cryptotenella*.62	0.311086	0.015	*Reimeria sinuata*.62	0.516829	0.045
14	NA 72	0.306287	0.015	*Gomphonema* cf. *angustatum*.5	0.506753	0.035
15	NA 444	0.288443	0.045	*Diatoma hyemalis*.3	0.487698	0.035
16	NA 310	0.254	0.045	NA 446	0.481227	0.02
17	NA 476	0.254	0.04	*Caloneis fontinalis*.2	0.481227	0.01
18	NA 563	0.254	0.04	*Fistulifera saprophila*.11	0.472727	0.02
19	NA 596	0.254	0.045	*Mayamaea lacunolaciniata*.9	0.470162	0.035
20	NA 629	0.254	0.045	NA 445	0.470162	0.025

Table 5: *Indicator Species Analysis results for top 20 species most strongly associated with glacier-fed streams [GFS] and tributaries [TRIBs] based on rbcL data.*

	***rbc*L GFSs**			***rbc*L TRIBs**		
	ASV	**stat**	**p.value**	**ASV**	**stat**	**p.value**
1	*Achnanthidium minutissimum*.56	0.667998	0.01	*Encyonema minutum*.5	0.787255	0.005
2	*Mayamaea permitis*.19	0.61657	0.005	*Psammothidium daonense*.7	0.739801	0.005
3	*Encyonopsis* sp.16	0.509421	0.005	*Psammothidium* sp.5	0.71166	0.015
4	*Encyonopsis* sp.3	0.463304	0.005	*Encyonema silesiacum*.8	0.699198	0.005
5	Gomphonema *micropus*.13	0.447214	0.005	*Planothidium frequentissimum*.2	0.683092	0.005
6	*Achnanthidium minutissimum*.11	0.445614	0.015	*Adlafia minuscula*.1	0.673984	0.005
7	*Encyonopsis falaisensis*.8	0.441819	0.03	*Reimeria sinuata*.15	0.672631	0.01
8	NA 170	0.40874	0.02	*Planothidium lanceolatum*	0.663015	0.015
9	NA 55	0.401609	0.015	*Navicula* sp..5	0.655282	0.01
10	*Encyonopsis* sp.24	0.4	0.005	NA 163	0.626406	0.01
11	*Pinularia Pinnularia* sp.5	0.395246	0.02	*Gomphonema saprophilum*.1	0.56815	0.005
12	*Psammothidium pseudoswazi*.8	0.370189	0.005	*Denticula tenuis*.2	0.560355	0.04
13	NA 157	0.366893	0.015	*Nitzschia* cf. *soratensis*.1	0.543233	0.005
14	*Fragilaria* sp. 2	0.363063	0.025	*Fistulifera saprophila*.2	0.525238	0.005
15	*Psammothidium pseudoswazi*.6	0.346106	0.01	*Rossithidium anastasiae*.4	0.521889	0.02
16	*Mayamaea permitis*.10	0.342916	0.025	*Encyonema minutum*.1	0.518448	0.01
17	*Adlafia minuscula*.8	0.340183	0.04	*Nitzschia alicae*.1	0.512639	0.005
18	*Nitzschia* cf. *pusilla*.3	0.338869	0.01	*Nitzschia* sp..2	0.510757	0.005
19	*Pinnularia* sp.11	0.338178	0.025	*Navicula radiosa*	0.500029	0.02
20	*Sellaphora saugerresii*.4	0.337497	0.03	*Amphora pediculus*	0.494981	0.03

4 Discussion

4.1 Taxonomical Evaluation

Besides addressing the main questions and hypotheses of this study, an initial overview was conducted to provide insight into the taxonomic composition of diatom communities across the sampled streams, evaluate the comparability of our findings with other studies in this field, and assess the consistency between the methods used in taxonomic identification.

4.1.1 Diatom taxa Composition

The number of taxa identified by the molecular methods (42 genera and 103 species for 18S, and 55 and 139 for *rbc*L) across the sampled floodplains was comparable with findings from other studies of GFSs in the Alps (Fell et al., 2018; Bert et al., 2024) and Canadian alpine streams (Gesierich and Rott, 2012). Most of the genera identified as dominant in this study (by all three of our methods; *Achnanthidium*, *Encyonema*, *Psammothidium*, *Navicula* and *Nitzschia*) were also reported to dominate alpine streams in other studies (Bona et al., 2012; Gesierich and Rott, 2012; Fell et al., 2018; Bert et al., 2024). The most notable difference was that while most other studies report *Achnanthidium* as the most dominant genus, usually with *A. minutissimum* as the most common species, we also found the genus *Reimeria* to be well-represented Bert et al. (2024).

Achnanthidium minutissimum and *Reimeria sinuata* are ecologically equivalent species known from a wide variety of streams (Fránková et al., 2009; Fell et al., 2018), and both have complex nomenclatural histories. *Reimeria sinuata* was previously moved from the genus *Cymbella* (Kociolek and Stoermer, 1987) and has not generally been reported from high-altitude streams despite its widespread distribution (Fránková et al., 2009; Morales et al., 2009; Kociolek, 2018). *Achnanthidium minutissimum*, on the other hand, is known to be a widely dominant generalist species in alpine regions worldwide thanks to its variety of ecomorphs that are able to grow on highly disturbed substrates in oligotrophic, cold water (Kawecka and Robinson, 2008; Gesierich and Rott, 2012; Bert et al., 2024). However, its nomenclatural history is even more complicated. Due to its small dimensions and high intraspecific morphological variation (which complicate morphological analysis considerably), the taxonomic hierarchy and classification of this species were frequently changed throughout history, ultimately resulting in the recognition of *A. minutissimum* as a cryptic species complex in need of taxonomic revision (Potapova and Hamilton, 2007; Bert et al., 2024).

Another frequently observed genus in our study was *Denticula tenuis.* While not generally common in other alpine stream studies, *D. tenuis* was previously found to be dominant in lake outlets in a study of Swiss Alpine streams (Hieber et al., 2001). Yet, it is worth noting that in our samples, most individuals of this genus were associated with a single glacier floodplain (i.e., SOY). This suggests that while there are certain trends in the community composition of alpine streams worldwide, local conditions, stochastic factors, and applied classification systems continue to play an important role in reported community compositions. Furthermore, changes in glacial input to catchments have already affected, and will likely continue to reshape, diatom assemblages in GFSs (Fell et al., 2018), further increasing the differences between past and future studies.

4.1.2 Comparison of Different Identification Approaches

Three identification methods were applied (i.e. morphology, *rbc*L, and 18S) to characterize diatom community structure, and simultaneously revealed insight into the current challenges in diatom classification. Therefore, we also sought to examine the strengths and limitations associated with each method, particularly in the context of biomass- and species-poor environments such as GFSs. Differences between the three methods were evident from the outset when comparing identified genera in the dataset of 18 TRIB samples where all three methods were applied: *rbc*L identified the highest number of genera (42), followed by 18S (37), and LM (35). Although of course these values are not identical, they are remarkably similar to each other all things considered.

Examining the composition of these samples, we found that each method assigns varying levels of importance to different taxa. These discrepancies arise from the distinct limitations of each approach. LM was constrained not only by the low abundances of diatoms and high debris concentrations, as previously mentioned, but also the prevalence of very small taxa (e.g. *Achnanthidium* spp.), which are difficult to identify morphologically. Furthermore, certain taxa, such as larger species of *Navicula* or *Hannaea*, appeared more susceptible to damage during preparation, further complicating their morphology-based identification.

On the other hand, both the 18S and *rbc*L barcoding methods are unaffected by high debris concentrations, low cell abundance, and damaged frustules (Fišer Pečnikar and Buzan, 2014; Kabiraj et al., 2022), thus allowing them to detect the presence of diatoms even where the morphological methods would fail. However, both these markers have their own caveats and limitations, as evidenced by the discrepancies between their results. For example, 18S results showed a higher degree of taxonomic resolution (containing almost three times as many ASVs assigned to more or less similar numbers of species and genera as in *rbc*L), meaning that it detected more of the intraspecific variation than *rbc*L. However, at the levels of species and genera, *rbc*L revealed slightly more taxa, which is caused in part by superior reference database (see *Introduction*), and in part by relatively low confidence threshold of 40%, which seems to enhance *rbc*L-based numbers faster than those obtained through 18S (e.g., when compared to a taxonomic assignment utilizing a default 70% confidence threshold, *rbc*L raised from 48 to 55 genera, while 18S raised only from 40 to 42). In addition, *rbc*L allowed for the more complete utilization of the dataset, leaving only 2.7% of the reads unassigned at the species level, while 18S left a full quarter of the reads unassigned.

Aside from the already mentioned distinct reference databases, part of the differences in taxonomic evaluation across sequencing methods can be attributed to the fundamental differences between the barcodes. While the *rbc*L gene codes for a protein, and is therefore more conserved, the 18S rDNA encodes the rRNA composing the small ribosomal subunit, and thus contains hypervariable loop regions that are not subject to purifying selection, leading to a greater variability of the marker and potentially also intraspecific resolution (Zimmermann et al., 2011; Kollár et al., 2021; Kabiraj et al., 2022). Another important factor is that the 18S data in this study were not obtained with diatom-specific 18S primers, but rather via general microeukaryotic TAR primers (Shi et al., 2022) with lower specificity to diatoms, which could explain its lower taxonomic resolution compared to the *rbc*L data, which were obtained with primers designed specifically for diatoms (Vasselon et al., 2017). Collectively, these results clearly suggest that the most accurate and complete insight into the taxonomic structure of diatom communities is achieved by combining both molecular and morphological approaches.

4.2 Environmental and Spatial Factors

Having established a general understanding of the diatom communities present in our streams, we now turn to addressing our first main question: do diatom species compositions significantly differ between glacier floodplains and contrasting stream types? Based on our knowledge from previous studies, we hypothesized that both the glacier floodplain and stream type of origin would significantly influence community structure, with stream type having the greatest influence. While the analysis confirmed the significance of both factors, it revealed that the glacier floodplain had a stronger influence than initially expected.

4.2.1 The Effect of Glacial Floodplains

The glacier floodplain of origin significantly shaped the diatom community composition in our data. Even if uneven dispersions may have had an influence on this result, more variability overall seems to be explained by the location than by the stream type. While diatom and other algal communities are known to be influenced by catchment characteristics such as geomorphology, altitude, and local weather conditions (Gesierich and Rott, 2012; Fell et al., 2018), a previous study from Canadian mountains reported similar diatom composition even between sites with fundamentally different geological conditions and glacier sizes (Gesierich and Rott 2012). Instead, that study identified the distance from the glacier as the primary factor influencing diatom communities, which was not the case for our data as discussed later.

We speculate that the floodplain influence is due to two main factors: differences in water properties (e.g. environmental filtering) and spatial structuring (e.g. dispersal limitation). The distinct clustering of SOY in the PCoA supports this, as SOY has the most unique water properties among the floodplains, including lower temperatures and higher levels of alkalinity, conductivity, and turbidity. Furthermore, spatial factors have been previously found responsible for 20 – 30% of the variation in diatom communities in freshwater lakes and streams on intermediate and regional scales (Soininen, 2007). However, while SOY clustered separately, it was the VAR glacier floodplain that was more geographically distant—approximately 200 km from the other two glaciers, which are themselves separated by only 15 km. This would suggest that, in this case, environmental factors have a stronger influence on alpine diatom community composition than spatial separation.

4.2.2 The Effect of Stream Types

Along with glacier floodplain, stream type significantly influenced diatom community structure, although with less variability explained. Within individual glacier subsets, the distinctions between stream types appeared clearer. Interestingly, for the VAR glacier floodplain, stream type did not emerge as a significant factor in shaping the community composition in 18S data. This could be due to the relatively underdeveloped TRIB area in VAR, which may reduce the contrast between stream types. However, the *rbc*L data still reflected differences between stream types, even under these conditions, further emphasizing the contrasting outcomes of the two barcoding methods.

The role of stream type in shaping benthic diatom communities may become even more pronounced in the upcoming years as the intensity of glacier melt escalates, leading to increased glacier meltwater input further intensifying the already harsh conditions of GFSs (Sudlow et al., 2023). After reaching the maximum melt rate known as “peak water”, glacier meltwater input is expected to decline until it ceases completely. In streams supported by sufficient precipitation and groundwater, differences may gradually weaken, creating conditions comparable to non-glacier-fed streams and allowing for the development of similar diatom communities. Conversely, streams lacking alternative water sources might disappear or become seasonally intermittent, intensifying the contrasts between sites (Fell et al., 2018; Huss and Hock, 2018; Sudlow et al., 2023).

4.3 Glacial Impact on Diatom Diversity

Given past results for bacteria and the overall eukaryote community (Brandani et al., 2022), we hypothesized lower alpha diversity for diatom communities in GFSs compared to TRIBs. Indeed, we found this confirmed across all floodplains and datasets. The negative effect of glacial influence on diatom alpha diversity has been previously reported in other studies of stream diatoms (e.g. Gesierich and Rott, 2012; Thies et al., 2013; Fell et al., 2018; Bert et al., 2024). Conversely, Robinson and Kawecka (2005) did not observe a significant difference in average species richness when comparing two Swiss basins—one dominated by glacial melt input and the other by precipitation. However, it is important to note that in their study differences in average species richness across entire basins rather than stream segments with varying degrees of glacial influence were compared.

It is generally assumed that the low algal richness in streams with high glacial meltwater input is due to the specific conditions of these habitats, such as low temperature, high discharge, turbidity, and low organic concentrations (Robinson and Kawecka, 2005; Thies et al., 2013; Fell et al., 2018). These challenging conditions demand specific cell adaptations for survival, filtering out loosely attached or tall algae (Sudlow et al., 2023). Furthermore, frequent physical disturbances prevent diatom and other algal communities from reaching a mature ‘climax’ stage, thereby maintaining density and diversity in such streams (Bona et al., 2012). In the future, as glacial influence diminishes, and conditions become less severe, alpha diversity in former GFSs is expected to increase, as the reduction in environmental stressors and disturbances will enable the expansion of species that were previously unable to persist in the harsh glacial environment (Fell et al., 2018).

4.4 Community Similarity

For the presence-absence based comparison we expected the ASV composition to be more similar between different stream types within the same floodplain than between the same stream types of different floodplains. This presumption was partly made based on previous research (Fell et al., 2018) and partly on the characteristics of the floodplains’ stream web, where the TRIBs flow out into the GFSs, which enhances the probability of encountering species washed out of their desired habitat.

The UpSet plots illustrating the distribution of ASVs across all six subsets demonstrated that the majority of ASVs were restricted to a single stream type within a single glacier floodplain. This specificity of some taxa to a single location does not seem to be uncommon as in other studies (Gesierich and Rott, 2012; Fell et al., 2018), as a high proportion of identified diatom species was found to be present in one sample only.

The higher numbers of ASVs shared between sample sets of the same floodplain compared to those of the same stream type align with the previously observed stronger influence of floodplain location on community composition. The overall higher count of ASVs in TRIBs corresponds to the higher alpha diversity averages observed in these stream types. However, the disproportionately high ASV count in the GFS SOY subset of the *rbc*L data was unexpected. Given that the median alpha diversity of GFS samples was lower than that of TRIB samples in this catchment, we speculate that this high ASV count may result from greater variability among the samples within this subset.

Consistent with the UpSet plot, the Jaccard matrix revealed a high level of similarity for same-floodplain pairs. However, unlike the UpSet plot, SOY stream types appeared less similar than the other glacier pairs. Interestingly, the *rbc*L dataset displayed much higher similarity values for stream type pairs within the same catchment than 18S. This observation contrasts with its previously demonstrated ability to distinguish between these subsets in PCoA and PERMANOVA analyses. This discrepancy may be partly explained by the use of Jaccard distances in this analysis, which focuses solely on presence-absence data, compared to Bray-Curtis dissimilarities used in previous analyses that also account for relative abundances. The reliance on presence-absence data in Jaccard-based evaluations might highlight *rbc*L's tendency to capture a core set of widely distributed taxa, resulting in higher similarity values between stream type pairs. In contrast, Bray-Curtis dissimilarities likely emphasize dominant taxa and abundance patterns, better reflecting the ecological drivers shaping community structure.

The findings from the UpSet plots, Jaccard similarity matrix, and previous analyses suggest that similarity between TRIBs and GFSs within the same floodplain is likely to increase over time as glacial retreat progresses and GFSs transition to more stable conditions resembling TRIBs. In contrast, the similarity between different glacier floodplains is not expected to change significantly, as spatial factors and environmental conditions of each catchment will continue to maintain distinct community structures across catchments.

4.5 Stream-type Associated Taxa

Identifying species associated with specific stream types is crucial for predicting future shifts in diatom community composition within changing floodplains. We hypothesised that while there will be more species associated with TRIBs, specialists in the vanishing GFSs will also be present. Along with testing our hypothesis by Indicator Species Analysis, we used bubble plots to gain an overview of general preferences of diatom genera across stream types and floodplains.

From the bubble plots representing the genera-level composition of all six sample subsets (i.e. floodplain vs. stream type), it was observed that the most abundant genera, such as *Achnanthidium*, *Reimeria*, *Navicula*, *Psammothidium*, and *Encyonema*, were present across all subsets and methods. These genera have also been recognized as generalist taxa found across multiple stream types in previous studies (Cantonati et al., 2001; Hieber et al., 2001; Gesierich and Rott, 2012), with the exception of *Reimeria*, which has been identified as preferentially associated with low-glacial input streams (Fell et al., 2018; Bert et al., 2024). Less abundant genera, such as *Sellaphora*, *Geissleria*, and *Caloneis*, exhibited preferences for specific floodplains and often varied depending on the identification method. Consistent with earlier findings, the genera composing the SOY glacier floodplain differed notably from the other two.

While no clear stream-type preferences for any genera were recognised from the bubble plots, this limitation was addressed through the implementation of the Indicator Species Analysis. In this analysis, individual ASVs characteristic for a particular glacial floodplain and/or stream type were identified. Interestingly, while more ASVs were identified as being characteristic for individual floodplains using the 18S dataset, the *rbc*L dataset revealed more ASVs characteristic of a given stream type. In both datasets, a consistently greater number of ASVs were significantly associated with TRIBs, aligning with the higher alpha diversity observed for this stream type, given the stricter filtering effect of the GFSs due to their harsh environmental characteristics, as previously discussed. Notably, except for ASVs from the *Achnanthidium minutissimum* complex, other species such as *Diatoma mesodon*, *Hannaea arcus*, and *Meridion circulare*—taxa that are commonly recognized in other studies as representative of streams with the highest glacier input (Hieber et al., 2001; Robinson and Kawecka, 2005; Kawecka and Robinson, 2008; Gesierich and Rott, 2012; Bert et al., 2024)—were not given the same status in our data. Conversely, taxa previously associated with low glacial influence in these same studies, such as *Mayamaea permitis*, *Navicula cryptotenella*, and *Reimeria sinuata*, were found to be characteristically associated with GFSs in our study.

The use of ASVs instead of species in this analysis, along with incomplete database entries, resulted in a significant number of unidentified taxa, underscoring the challenge of fully capturing biodiversity. Furthermore, some species were associated with multiple stream types, reflecting the cryptic diversity within these groups. Despite these challenges, identifying taxa specific to streams with high glacial input remains critical due to the vulnerability of this habitat type to glacier retreat.

Among the species strongly associated with TRIBs, one (*Encyonema silesiacum*) was classified as extremely rare, one (*Psammothidium daonense*) as under a threat of unknown extent, and another (*Nitzschia acidoclinata*) was included on the watchlist in the Diatom Red List of Germany (Hofmann, 2018). In GFSs, three species—*Encyonopsis falaisensis*, *Pinnularia subcommutata*, and *Pinnularia subcommutata* var. *nonfasciata*—were also identified as under a threat of unknown extent. Considering the number of unidentified taxa and species not included on the list, it is likely that the actual number of endangered or threatened species is considerably higher, which is especially important for the GFSs.

This concern is underscored by Fell et al. (2018), who identified six diatom species exclusive to high-glacial input sites that were absent from the Diatom Red List of Germany. Such findings highlight the need for a reclassification of endangered diatom species, especially as these glacial specialists are among the most threatened by glacier retreat driven by global warming. In contrast, the expansion of the more stable habitats of precipitation- and groundwater-fed streams could provide a refuge for endangered and rare diatom taxa specifically associated with these stream types. These taxa currently appear to outnumber the endangered or rare species specialized for GFSs (Fel et al., 2018; Bert et al., 2024).

5 Synthesis and Outlook

5.1 Key Findings and Implications

This study set out to explore the impacts of glacier retreat on diatom communities inhabiting the streams of alpine floodplains, combining traditional morphological and molecular methods to provide a comprehensive understanding of these fragile ecosystems. By examining diatom assemblages in both glacier-fed streams (GFSs) and their non-glacial tributaries (TRIBs) across three Alpine floodplains in Switzerland, we captured the dynamic interplay between community structure and environmental change.

Our study suggests that: **a)** both stream type and floodplain location significantly influence diatom communities, with location likely providing the first and stream type the second environmental filter for the diatom flora; **b)** TRIBs exhibit significantly higher diatom diversity compared to GFSs, likely due to their more 'relaxed' environmental conditions and reduced frequency and magnitude of disturbances; and **c)** species composition is more similar between both stream types within the same glacial floodplain than between different glacial floodplains of the same stream type, emphasizing the role of localized factors. Lastly, **d)** Indicator Species Analysis identified distinct taxa associated with each stream type, with TRIBs hosting a greater number of ASVs characteristic of this habitat type than GFSs. Finally, **e)** while different identification methods (i.e. morphology, 18S, *rbc*L) showed consistent trends at the community level, they revealed discrepancies in taxonomic identification and resolution, highlighting the limitations of individual approaches and the value of combining techniques to achieve the most accurate and comprehensive picture of diatom communities.

5.2 Current and Future state of Glacial Floodplains

Based on this research and other investigations on this topic, we suggest that streams with high glacial influence are primarily dominated by pioneer species characterized by high resilience. These taxa exhibit traits such as low-profile growth forms, motility, strong attachment to substrates, small sizes and quick grow rates, which enhance their ability to recolonize streams rapidly following frequent disturbances (Hieber et al., 2001; Sudlow et al., 2023; Bert et al., 2024). Many of these species, such as those from the genera *Achnanthidium*, *Psammothidium*, *Encyonema*, *Fragilaria*, and *Gomphonema*, are generalists that are also present in non-glacial streams. In contrast, a smaller number of specialist taxa, which are strictly adapted to GFS conditions, were identified, including *Mayamaea permitis*, *Nitzschia pusilla*, and *Encyonopsis falaisensis* in our study (Gesierich and Rott, 2012; Fell et al., 2018).

Non-glacial streams, on the other hand, tend to host a greater variety of loosely attached taxa with higher motility, larger cell sizes, and lower resistance to strong flow conditions. Examples include species from the genera *Nitzschia* and *Navicula*, which were often absent from GFSs (Hieber et al., 2001; Sudlow et al., 2023; Bert et al., 2024). As the conditions of GFSs are expected to shift toward those of non-glacial streams due to glacier retreat, these non-glacial taxa are anticipated to spread and potentially outcompete GFS specialists. This expansion of non-glacial specialist species is likely to increase alpha diversity within streams; however, the replacement of glacial specialists with non-glacial taxa will likely reduce beta diversity between stream types (Fell et al., 2018). Other studies investigating abundance have also reported an overall increase in diatom and algal density with decreasing meltwater input (Hieber et al., 2001; Rott et al., 2006; Fell et al., 2018).

Changes in the volume and composition of primary producers could have cascading effects on higher trophic levels (Sudlow et al., 2023). The positive impact of glacier recession on alpha diversity has also been documented in other components of the stream food web, including microbes, bacteria, other algae, macroinvertebrates, nematodes, and rotifers (Rott et al., 2006; Wilhelm et al., 2013; Fell et al., 2018; Brandani et al., 2022). This suggests that either different trophic levels exhibit similar responses to decreasing glacier input or that food web connections in these ecosystems are particularly strong (Fell et al., 2018).

5.3 Complicating Factors and Uncertainties

The future state of glacial floodplains will depend on other numerous factors, many of which are difficult to predict. A notable proportion of streams may dry out or exhibit intermittent flows, potentially reducing species diversity or selecting for organisms with desiccation resistance (Kawecka and Robinson, 2008; Sudlow et al., 2023). Additionally, the expected reduction in the movement of so-called glacial flour (i.e. fine particles grazed off the surrounding rocks by glacier movement) could lower phosphorus and nitrogen inputs into the stream network, making some nutrients less accessible (Sudlow et al., 2023). Although Fell et al. (2018) did not find a significant correlation between taxonomic richness and NO_3 or DOC, broader shifts in nutrient cycling could still alter the ecological functions that diatoms and other algae provide within the food web (Sudlow et al., 2023). For instance, epilithic algae in harsh glacial streams have been found to exhibit higher nutritional quality compared to those in more moderate streams (Niedrist et al., 2018). However, this difference may be partially offset by the higher algal biomass typically observed in non-glacial streams. At the same time, changes in water quality driven by glacial recession could create favourable conditions for algal blooms, such as those of *Didymosphenia geminata* (Brahney et al., 2021; Bert et al., 2024).

Making predictions about the effects of reduced glacial input is further complicated by the interplay of local weather conditions, seasonal patterns, geological factors, and pure spatial effects, all of which vary significantly across different locations (Hieber et al., 2001; Fell et al., 2018; Sudlow et al., 2023). Our study has demonstrated a strong influence of location, even at relatively small spatial scales. Moreover, differences in glacier ablation rates, driven by these environmental conditions, mean that changes will occur at varying paces across different regions, potentially altering the ecological outcomes (Fell et al., 2018).

Altogether, these factors make identifying general patterns in global alpine floodplains challenging. The complexity of interacting variables underscores the need for localized studies and adaptive conservation strategies tailored to the unique conditions of each floodplain.

5.4 Comparison of Identification Methods

Building on the insights gained from our analysis, it is clear that each identification approach offers distinct advantages and faces specific limitations. DNA barcoding methods, in general, provide a relatively low-cost, time-efficient tool capable of identifying species from minimal amount of samples. These methods excel in handling large datasets and are invaluable for uncovering hidden biodiversity, particularly by distinguishing cryptic species (Fišer Pečnikar and Buzan, 2014; Hubert and Hanner, 2015; Kabiraj et al., 2022). However, their effectiveness is constrained by incomplete reference databases—an issue particularly pronounced in diatoms, where many species have not been successfully cultured—and by the current inability to achieve 100% taxonomic accuracy, especially given the complex species concept and phenotypic plasticity in algae (Hebert and Gregory, 2005; Fišer Pečnikar and Buzan, 2014; DeSalle and Goldstein, 2019; Kabiraj et al., 2022).

Morphological identification, while limited by its dependence on specialized taxonomists, time-consuming procedures, and inability to distinguish cryptic species, offers unique advantages. As demonstrated in our study, it requires high-quality samples but allows for the recognition of additional traits such as cell size, motility, viability, and the precise location of organisms at the time of sampling (Fišer Pečnikar and Buzan, 2014; Rees et al., 2014; Kabiraj et al., 2022). These insights are critical for understanding diatom ecology and their roles within stream environments.

Our results highlight the complementary nature of these approaches. While the 18S barcoding method detected the highest number of ASVs and demonstrated strong resolution at this level, *rbc*L barcoding identified more taxa at the genus and species levels and showed better differentiation between stream types. Morphological identification, despite its limitations in stream type comparisons, proved crucial for setting the confidence thresholds for molecular methods, ensuring that taxonomic assessments reflect true community compositions as closely as possible. However, the comparison of methods in our study was limited by analysing only a small subset of the total samples, which may influence the generalizability of these findings and underscores the need for further comprehensive evaluations.

5.5 Future Prospects

Looking forward, our findings provide a solid foundation for understanding the ecological impacts of glacier retreat on diatom communities in alpine floodplains, yet they also highlight critical areas for future research. A key priority should be the supplementation of reference libraries to address the limitations of DNA barcoding, particularly for diatoms, many of which remain uncultured and undescribed. Special attention should be given to identifying and characterizing the currently unidentified species unique to glacier-fed streams, as understanding their ecological roles is crucial for assessing the impacts of glacial loss. Furthermore, this study emphasizes the importance of combining morphological and molecular methods in similar assessments of diatom communities, as this integrative approach provides the most accurate and comprehensive results. Finally, exploring the relationships between diatoms and other components of the stream food web, such as microbes, macroinvertebrates, and higher trophic levels, will be essential to fully grasp the cascading ecological effects of glacial meltwater reduction. By addressing these priorities, future research can further unravel the complexities of alpine stream ecosystems and contribute to their conservation in the face of rapid environmental change.

References

Amaral-Zettler, L. A., E. A. McCliment, H. W. Ducklow, and S. M. Huse. 2009. A method for studying protistan diversity using massively parallel sequencing of V9 hypervariable regions of small-subunit ribosomal RNA genes. *PloS one* 4: e6372.

Barnett, D. J. M., I. C. W. Arts, and J. Penders. 2021. microViz: an R package for microbiome data visualization and statistics.

Bert, M., E. Falasco, L. Mobili, S. Piovano, and F. Bona. 2024. Diatom assemblages in glacial-fed streams of Italian Western Alps. *Botany Letters*: 1–17.

Bey, M. Y., and L. Ector. 2013. Atlas des diatomées des cours d'eau de la région Rhône-Alpes, Tome 1-6. *DREAL Rhône-Alpes*.

Bisanz, J. E. 2018. qiime2R: Importing QIIME2 artifacts and associated data into R sessions.

Bokulich, N. A., B. D. Kaehler, J. R. Rideout, M. Dillon, E. Bolyen, R. Knight, G. A. Huttley, and J. Gregory Caporaso. 2018. Optimizing taxonomic classification of marker-gene amplicon sequences with QIIME 2's q2-feature-classifier plugin. *Microbiome* 6: 90.

Bolyen, E., J. R. Rideout, M. R. Dillon, N. A. Bokulich, C. C. Abnet, G. A. Al-Ghalith, H. Alexander, et al. 2019. Reproducible, interactive, scalable and extensible microbiome data science using QIIME 2. *Nature biotechnology* 37: 852–857.

Bona, F., V. La Morgia, and E. Falasco. 2012. Predicting River Diatom Removal After Shear Stress Induced by Ice Melting. *River Research and Applications* 28: 1289–1298.

Bosson, J. B., M. Huss, S. Cauvy-Fraunié, J. C. Clément, G. Costes, M. Fischer, J. Poulenard, and F. Arthaud. 2023. Future emergence of new ecosystems caused by glacial retreat. *Nature* 620: 562–569.

Brahney, J., M. L. Bothwell, L. Capito, C. A. Gray, S. E. Null, B. Menounos, and P. J. Curtis. 2021. Glacier recession alters stream water quality characteristics facilitating bloom formation in the benthic diatom *Didymosphenia geminata*. *Science of The Total Environment* 764: 142856.

Brandani, J., H. Peter, S. B. Busi, T. J. Kohler, S. Fodelianakis, L. Ezzat, G. Michoud, et al. 2022. Spatial patterns of benthic biofilm diversity among streams draining proglacial floodplains. *Frontiers in Microbiology* 13.

Brandani, J., H. Peter, S. Fodelianakis, T. J. Kohler, M. Bourquin, G. Michoud, S. B. Busi, et al. 2023. Homogeneous Environmental Selection Structures the Bacterial Communities of Benthic Biofilms in Proglacial Floodplain Streams. *Applied and Environmental Microbiology* 89: e02010-22.

Bray, J. R., and J. T. Curtis. 1957. An ordination of the upland forest communities of southern Wisconsin. *Ecological monographs* 27: 326–349.

Brittain, J. E., and A. M. Milner. 2001. Ecology of glacier-fed rivers: current status and concepts. *Freshwater Biology* 46: 1571–1578.

Brown, L. E., D. M. Hannah, and A. M. Milner. 2003. Alpine Stream Habitat Classification: An Alternative Approach Incorporating the Role of Dynamic Water Source Contributions. *Arctic, Antarctic, and Alpine Research* 35: 313–322.

Busi, S. B., H. Peter, J. Brandani, T. J. Kohler, S. Fodelianakis, P. Pramateftaki, M. Bourquin, et al. 2024. Cross-domain interactions confer stability to benthic biofilms in proglacial streams. *Frontiers in Microbiomes* 2.

Busi, S. B., P. Pramateftaki, J. Brandani, S. Fodelianakis, H. Peter, R. Halder, P. Wilmes, and T. J. Battin. 2020. Optimised biomolecular extraction for metagenomic analysis of microbial biofilms from high-mountain streams. *PeerJ* 8: e9973.

Cáceres, M. D., and P. Legendre. 2009. Associations between species and groups of sites: indices and statistical inference. *Ecology* 90: 3566–3574.

Callahan, B. J., P. J. McMurdie, M. J. Rosen, A. W. Han, A. J. A. Johnson, and S. P. Holmes. 2016. DADA2: High-resolution sample inference from Illumina amplicon data. *Nature methods* 13: 581–583.

Cantonati, M., C. G, I. Jüttner, and E. Cox. 2001. Diatom assemblages in high mountain streams of the Alps and the Himalaya. *Nova Hedwigia* 123: 37–62.

Clitherow, L. R., J. L. Carrivick, and L. E. Brown. 2013. Food Web Structure in a Harsh Glacier-Fed River. *PLOS ONE* 8: e60899.

De Tommasi, E., J. Gielis, and A. Rogato. 2017. Diatom Frustule Morphogenesis and Function: a Multidisciplinary Survey. *Marine Genomics* 35: 1–18.

De Vargas, C., S. Audic, N. Henry, J. Decelle, F. Mahé, R. Logares, E. Lara, et al. 2015. Eukaryotic plankton diversity in the sunlit ocean. *Science* 348: 1261605.

DeSalle, R., and P. Goldstein. 2019. Review and Interpretation of Trends in DNA Barcoding. *Frontiers in Ecology and Evolution* 7.

Fell, S. C., J. L. Carrivick, M. G. Kelly, L. Füreder, and L. E. Brown. 2018. Declining glacier cover threatens the biodiversity of alpine river diatom assemblages. *Global Change Biology* 24: 5828–5840.

Fišer Pečnikar, Ž., and E. V. Buzan. 2014. 20 years since the introduction of DNA barcoding: from theory to application. *Journal of Applied Genetics* 55: 43–52.

Fránková, M., A. Poulíčková, J. Neustupa, M. Pichrtová, and P. Marvan. 2009. Geometric morphometrics-a sensitive method to distinguish diatom morphospecies: a case study on the sympatric populations of Reimeria sinuata and Gomphonema tergestinum (Bacillariophyceae) from the River Becva Czech Republic. *Nova Hedwigia* 88: 81–95.

Füreder, L., and G. H. Niedrist. 2020. Glacial stream ecology: Structural and functional assets. *Water* 12: 376.

Garlapati, D., B. Charankumar, K. Ramu, P. Madeswaran, and M. V. Ramana Murthy. 2019. A review on the applications and recent advances in environmental DNA (eDNA) metagenomics. *Reviews in Environmental Science and Bio/Technology* 18: 389–411.

Gehlenborg, N. 2019. UpSetR: A More Scalable Alternative to Venn and Euler Diagrams for Visualizing Intersecting Sets.

Gesierich, D., and E. Rott. 2012. Is diatom richness responding to catchment glaciation? A case study from Canadian headwater streams. *Journal of Limnology* 71.

Guiry, M. D. 2024. How many species of algae are there? A reprise. Four kingdoms, 14 phyla, 63 classes and still growing. *Journal of Phycology* 60: 214–228.

Hebert, P. D., A. Cywinska, S. L. Ball, and J. R. deWaard. 2003. Biological identifications through DNA barcodes. *The Royal Society*. Website https://royalsocietypublishing.org/doi/epdf/10.1098/rspb.2002.2218 [accessed 10 October 2024].

Hebert, P. D., and T. R. Gregory. 2005. The promise of DNA barcoding for taxonomy. *Systematic biology* 54: 852–859.

Hieber, M., C. T. Robinson, S. R. Rushforth, and U. Uehlinger. 2001. Algal Communities Associated with Different Alpine Stream Types. *Arctic, Antarctic, and Alpine Research* 33: 447–456.

Hofmann, G. 2018. Hofmann: Rote Liste der limnischen Kieselalgen [Freshwate... - Google Scholar. Website https://scholar.google.com/scholar_lookup?&title=Rote%20Liste%20der%20limnischen%20Kieselalgen&journal=Naturschutz%20und%20Biologische%20Vielfalt&volume=70&issue=7&pages=601-708&publication_year=2018&author=Hofmann%2CG&author=Lange-Bertalot%2CH&author=Werum%2CM&author=Klee%2CR [accessed 5 November 2024].

Hollingsworth, P. M., L. L. Forrest, J. L. Spouge, M. Hajibabaei, S. Ratnasingham, M. van der Bank, M. W. Chase, et al. 2009. A DNA barcode for land plants. *Proceedings of the National Academy of Sciences* 106: 12794–12797.

Hubert, N., and R. Hanner. 2015. DNA barcoding, species delineation and taxonomy: a historical perspective. *DNA barcodes* 3.

Huss, M., and R. Hock. 2018. Global-scale hydrological response to future glacier mass loss. *Nature Climate Change* 8: 135–140.

Kabiraj, S., S. Bhuyan, and U. Goutam. 2022. Species Identification in Diatoms using DNA Barcoding: An Overview.

Kahlert, M., M. Kelly, R.-L. Albert, S. F. P. Almeida, T. Bešta, S. Blanco, M. Coste, et al. 2012. Identification versus counting protocols as sources of uncertainty in diatom-based ecological status assessments. *Hydrobiologia* 695: 109–124.

Kassambara, A. 2020. ggpubr:‘ggplot2’based publication ready plots. R package version 0.4. 0.

Kawecka, B., and C. Robinson. 2008. Diatom communities of lake/stream networks in the Tatra Mountains, Poland, and the Swiss Alps. *Oceanological and Hydrobiological Studies* 37: 21–35.

Kociolek, J. P. 2018. A worldwide listing and biogeography of freshwater diatom genera: a phylogenetic perspective. *Diatom Research* 33: 509–534.

Kociolek, J. P., and E. F. Stoermer. 1987. Ultrastructure of Cymbella sinuata and its Allies (Bacillariophyceae), and Their Transfer to Reimeria, Gen. Nov. *Systematic Botany* 12: 451–459.

Kollár, J., E. Pinseel, W. Vyverman, and A. Poulickova. 2021. A time-calibrated multi-gene phylogeny provides insights into the evolution, taxonomy and DNA barcoding of the Pinnularia gibba group (Bacillariophyta). *Fottea* 21: 62–72.

Kooistra, W. H., and L. K. Medlin. 1996. Evolution of the diatoms (Bacillariophyta): IV. A reconstruction of their age from small subunit rRNA coding regions and the fossil record. *Molecular phylogenetics and evolution* 6: 391–407.

Krammer, K. 1997. Die cymbelloiden Diatomeen: eine Monographie der weltweit bekannten Taxa. Cramer.

Krammer, K. 2000. The genus pinnularia. *Diatoms of Europe: diatoms of the European inland waters and comparable habitats* 1: 703.

Lahti, L., and S. Shetty. 2017. microbiome R package.

Lyon, B. R., and T. Mock. 2014. Polar microalgae: new approaches towards understanding adaptations to an extreme and changing environment. *Biology* 3: 56–80.

Mann, D. G., and K. M. Evans. 2008. The species concept and cryptic diversity. Proceedings of the 12th International Conference on Harmful Algae, 262–268. International Society for the Study of Harmful Algae and Intergovernmental ….

Mann, D. G., S. Sato, R. Trobajo, P. Vanormelingen, and C. Souffreau. 2010. DNA barcoding for species identification and discovery in diatoms. *Cryptogamie Algologie*.

Mann, D. G., and P. Vanormelingen. 2013. An Inordinate Fondness? The Number, Distributions, and Origins of Diatom Species. *Journal of Eukaryotic Microbiology* 60: 414–420.

Martin, M. 2011. Cutadapt removes adapter sequences from high-throughput sequencing reads. *EMBnet. journal* 17: 10–12.

McMurdie, P. J., and S. Holmes. 2013. phyloseq: An R package for reproducible interactive analysis and graphics of microbiome census data.

Medlin, L. K., and I. Kaczmarska. 2004. Evolution of the diatoms: V. Morphological and cytological support for the major clades and a taxonomic revision. *Phycologia* 43: 245–270.

Medlin, L. K., W. H. Kooistra, R. Gersonde, and U. Wellbrock. 1996. Evolution of the diatoms (Bacillariophyta). II. Nuclear-encoded small-subunit rRNA sequence comparisons confirm a paraphyletic origin for the centric diatoms. *Molecular Biology and Evolution* 13: 67–75.

Michoud, G., T. J. Kohler, H. Peter, J. Brandani, S. B. Busi, and T. J. Battin. 2023. Unexpected functional diversity of stream biofilms within and across proglacial floodplains despite close spatial proximity. *Limnology and Oceanography* 68: 2183–2194.

Mora, D., N. Abarca, S. Proft, J. H. Grau, N. Enke, J. Carmona, O. Skibbe, et al. 2019. Morphology and metabarcoding: a test with stream diatoms from Mexico highlights the complementarity of identification methods. *Freshwater Science* 38: 448–464.

Morales, E. A., E. Fernandez, and P. J. Kociolek. 2009. Epilithic diatoms (Bacillariophyta) from cloud forest and alpine streams in Bolivia, South America 3: diatoms from Sehuencas, Carrasco National Park, Department of Cochabamba. *Acta Botanica Croatica* 68: 263–283.

Mullis, K., F. Faloona, S. Scharf, R. Saiki, G. Horn, and H. Erlich. 1986. Specific enzymatic amplification of DNA in vitro: the polymerase chain reaction. Cold Spring Harbor symposia on quantitative biology, 263–273. Cold Spring Harbor Laboratory Press.

Niedrist, G. H., M. Cantonati, and L. Füreder. 2018. Environmental harshness mediates the quality of periphyton and chironomid body mass in alpine streams. *Freshwater Science* 37: 519–533.

Oksanen, J., G. L. Simpson, F. G. Blanchet, R. Kindt, P. Legendre, P. R. Minchin, R. B. O'Hara, et al. 2024. vegan: Community Ecology Package.

Pedersen, T. L. 2020. patchwork: The Composer of Plots. R package version 1.1. 1. *Website: https://CRAN. R-project. org/package= patchwork.*

Peter, H., G. Michoud, S. B. Busi, and T. J. Battin. 2024. The role of phages for microdiverse bacterial communities in proglacial stream biofilms. *Frontiers in Microbiomes* 2.

Pickett, S. T. A. 1989. Space-for-Time Substitution as an Alternative to Long-Term Studies. *In* G. E. Likens [ed.], Long-Term Studies in Ecology, 110–135. Springer New York, New York, NY.

Pinseel, E., S. B. Janssens, E. Verleyen, P. Vanormelingen, T. J. Kohler, E. M. Biersma, K. Sabbe, et al. 2020. Global radiation in a rare biosphere soil diatom. *Nature communications* 11: 2382.

Posit team. 2024. RStudio: Integrated Development Environment for R.

Potapova, M., and P. B. Hamilton. 2007. Morphological and Ecological Variation Within the Achnanthidium Minutissimum (bacillariophyceae) Species Complex. *Journal of Phycology* 43: 561–575.

Quast, C., E. Pruesse, P. Yilmaz, J. Gerken, T. Schweer, P. Yarza, J. Peplies, and F. O. Glöckner. 2012. The SILVA ribosomal RNA gene database project: improved data processing and web-based tools. *Nucleic acids research* 41: D590–D596.

R Core Team. 2024. R: A Language and Environment for Statistical Computing.

Rees, H. C., B. C. Maddison, D. J. Middleditch, J. R. M. Patmore, and K. C. Gough. 2014. REVIEW: The detection of aquatic animal species using environmental DNA – a review of eDNA as a survey tool in ecology E. Crispo [ed.],. *Journal of Applied Ecology* 51: 1450–1459.

Rimet, F., E. Gusev, M. Kahlert, M. G. Kelly, M. Kulikovskiy, Y. Maltsev, D. G. Mann, et al. 2019. Diat.barcode, an open-access curated barcode library for diatoms. *Scientific Reports* 9: 15116.

Robeson, M. S., D. R. O'Rourke, B. D. Kaehler, M. Ziemski, M. R. Dillon, J. T. Foster, and N. A. Bokulich. 2021. RESCRIPt: Reproducible sequence taxonomy reference database management. *PLoS computational biology* 17: e1009581.

Robinson, C. T., and B. Kawecka. 2005. Benthic diatoms of an Alpine stream/lake network in Switzerland. *Aquatic Sciences* 67: 492–506.

Rott, E., M. Cantonati, L. Füreder, and P. Pfister. 2006. Benthic Algae in High Altitude Streams of the Alps – a Neglected Component of the Aquatic Biota. *Hydrobiologia* 562: 195–216.

Rounce, D. R., R. Hock, F. Maussion, R. Hugonnet, W. Kochtitzky, M. Huss, E. Berthier, et al. 2023. Global glacier change in the 21st century: Every increase in temperature matters. *Science* 379: 78–83.

Round, F. E., R. M. Crawford, and D. G. Mann. 1990. Diatoms: biology and morphology of the genera. Cambridge university press.

Ruppert, K. M., R. J. Kline, and M. S. Rahman. 2019. Past, present, and future perspectives of environmental DNA (eDNA) metabarcoding: A systematic review in methods, monitoring, and applications of global eDNA. *Global Ecology and Conservation* 17: e00547.

Sarno, D., W. H. C. F. Kooistra, L. K. Medlin, I. Percopo, and A. Zingone. 2005. Diversity in the Genus *Skeletonema* (Bacillariophyceae). II. An Assessment of the Taxonomy of *S. costatum* -like Species with the Description of Four New Species[1]. *Journal of Phycology* 41: 151–176.

Shi, Z., Q. Kong, X. Li, W. Xu, C. Mao, Y. Wang, W. Song, and J. Huang. 2022. The Effects of DNA Extraction Kits and Primers on Prokaryotic and Eukaryotic Microbial Community in Freshwater Sediments. *Microorganisms* 10: 1213.

Soininen, J. 2007. Environmental and Spatial Control of Freshwater Diatoms—a Review. *Diatom Research* 22: 473–490.

Stoeck, T., D. Bass, M. Nebel, R. Christen, M. D. M. Jones, H.-W. Breiner, and T. A. Richards. 2010. Multiple marker parallel tag environmental DNA sequencing reveals a highly complex eukaryotic community in marine anoxic water. *Molecular Ecology* 19: 21–31.

Sudlow, K., S. S. Tremblay, and R. D. Vinebrooke. 2023. Glacial stream ecosystems and epilithic algal communities under a warming climate. *Environmental Reviews* 31: 471–483.

Thies, H., U. Nickus, M. Tolotti, R. Tessadri, and K. Krainer. 2013. Evidence of rock glacier melt impacts on water chemistry and diatoms in high mountain streams. *Cold Regions Science and Technology* 96: 77–85.

Vasselon, V., F. Rimet, K. Tapolczai, and A. Bouchez. 2017. Assessing ecological status with diatoms DNA metabarcoding: Scaling-up on a WFD monitoring network (Mayotte island, France). *Ecological Indicators* 82: 1–12.

Wang, Y., R. M. Tian, Z. M. Gao, S. Bougouffa, and P.-Y. Qian. 2014. Optimal eukaryotic 18S and universal 16S/18S ribosomal RNA primers and their application in a study of symbiosis. *PloS one* 9: e90053.

van der Werff, A. 1955. A new method of concentrating and cleaning diatoms and other organisms. *SIL Proceedings, 1922-2010* 12: 276–277.

Wickham, H. 2016. ggplot2: Elegant Graphics for Data Analysis.

Wickham, H., M. Çetinkaya-Rundel, and G. Grolemund. 2023. R for data science. O'Reilly Media, Inc.

Wilhelm, L., G. A. Singer, C. Fasching, T. J. Battin, and K. Besemer. 2013. Microbial biodiversity in glacier-fed streams. *The ISME Journal* 7: 1651–1660.

Yang, C., C. Feng, Y. Li, Z. Cao, Y. Sun, X. Li, L. Zhang, et al. 2023. Morphological and physicochemical characteristics, biological functions, and biomedical applications of diatom frustule. *Algal Research* 72: 103104.

Zeileis, A., J. C. Fisher, and K. Hornik. 2020. colorspace: A Toolbox for Manipulating and Assessing Colors and Palettes. Published online March 14, 2019.

Zemp, M., W. Haeberli, M. Hoelzle, and P. Frank. 2006. Alpine glaciers to disappear within decades? Website https://agupubs.onlinelibrary.wiley.com/doi/full/10.1029/2006GL026319 [accessed 10 April 2024].

Zimmermann, J., R. Jahn, and B. Gemeinholzer. 2011. Barcoding diatoms: evaluation of the V4 subregion on the 18S rRNA gene, including new primers and protocols. *Organisms Diversity & Evolution* 11: 173–192.